ABSTRACT

Title of Document: FUNCTIONAL CHARACTERIZATION OF THE VIRAL FLICE INHIBITORY PROTEIN OF RHESUS MONKEY RHADINOVIRUS

Krit Ritthipichai, MS, 2011

Directed By: Assistant Professor Yan-Jin Zhang, Department of Veterinary Medicine

Rhesus monkey rhadinovirus (RRV) is a gamma-2 herpesvirus closely related to Kaposi's sarcoma-associated herpesvirus (KSHV). KSHV is associated with several malignant diseases, including Kaposi's sarcoma, primary effusion lymphoma and multicentric Castleman's disease. Here we found that RRV viral FLICE inhibitory protein (vFLIP) inhibits apoptosis. In HeLa cells with vFLIP expression, cleavage of poly [ADP-ribose] polymerase 1 (PARP-1) and activities of caspase 3, 7, and 9 were much lower than controls. RRV vFLIP was able to enhance cell survival under starved condition or apoptosis induction. After apoptosis induction, autophagosome formation was enhanced in cells with vFLIP expression and when autophagy was inhibited, these cells underwent apoptosis. Moreover, RRV latent infection of BJAB B-lymphoblastoid cells protects the cells against apoptosis. Knockdown of vFLIP expression in the RRV-infected BJAB cells with siRNA abolished the protection against apoptosis. These findings indicate that RRV vFLIP protects cells against apoptosis by enhancing autophagosome formation.

FUNCTIONAL CHARACTERIZATION OF VIRAL FLICE INHIBITORY PROTEIN OF RHESUS MONKEY RHADINOVIRUS

By

Krit Ritthipichai

Thesis submitted to the Faculty of the Graduate School of the
University of Maryland, College Park, in partial fulfillment
of the requirement for the degree of
Master of Science
2011

Advisory Committee
Assistant Professor YanJin Zhang, Chair
Associate Professor Nathaniel Tablante
Assistant Professor Ioannis Bossis

Dedication

I wholedheartedly dedicate my work to my father, who inspired me to work on science, and my mother for her resepect and great support to my pursuing graduate studies.

Acknowledgement

I thank my advisor, Dr. Yan-Jin Zhang, for a great opportunity to join his lab and full support throughout my degree. These past couple of years in his lab will be one of the most memorable periods in my life. Under his generous guidance, I truly believe that I am fully prepared for the next important step in my life. I thank the members of my thesis committee: Drs. Nathaniel Tablante and Ioannis Bossis for their valuable recommendation and support throughout my graduate studies. I also thank my past and present lab members: Dr. Deendayal Patel, Dr. Sumin Fan, Dr. Harilakshmi Kannan, Meiyan Shen, Dr.Muhamad Mukhtar, Yuchen Nan, Brian Harriman, and Rong Wang for their sincere help.

I would have not made this day possible without your love, sacrifice, and encouragement. Thank you for your support when I move towards the directions that I have imagined.

Table of Contents

Dedication……...……....ii

Acknowledgements…….….iii

Table of contents……..……..…...iv

List of tables……..……vi

List of figures……..……..vii

List of abbreviations……..……...ix

Chapter 1: General introduction...…….....1

1.1 Introduction……...1
1.2 Research objectives……4

Chapter 2: Review of literature……5

2.1 Evolutionary and historical perspective of rhesus rhadinovirus ……...5

2.2 Biology of rhesus rhadinovirus ……..**.....**7

2.3 Viral FLICE inhibitory protein (vFLIP)……..……18

2.4 Apoptosis pathway……...22

2.5 Autophagy pathway……28

Chapter 3: Material and methods……..35

3.1 Cells and viruses……..35

3.2 Apoptosis and autophagy induction……36

3.3 Antibodies……...37

3.4 Plasmids and vectors……...38

3.5 Transfection……40

3.6 Confocal fluorescence microscopy…….…….....41

3.7 Western blot analysis……...41

3.8 Cell viability assay……...42

3.9 Activity assay of caspase-3,-7,-8, and -9……....42

3.10 NF-κB reporter assay……43

3.11 Subcellular fractionation……43

3.12 Design and tesing siRNA……...…44

3.13 Real-time PCR……...44

Chapter 4: Results……..……..46

4.1 Cloning and expression of RRV ORF71 gene…….46

4.2 RRV vFLIP inhibits apoptosis …….……...……48

4.3 RRV vFLIP does not activate NF-κB pathway……...52

4.4 Enhanced cell survival under starved condition in cells expressing vFLIP…….....55

4.5 Elevation of autophagosome formation in cells with RRV vFLIP expression after apoptosis induction……58

4.6 Inhibition of autophagic cell death induced by rapamycin treatment ……62

4.7 Truncated vFLIP proteins lose the roles of full-length vFLIP on apoptosis and autophagy pathway……64

4.8 RRV latent infection of BJAB cells protects the cells against apoptosis induction and suppression of vFLIP with siRNA abolishes the protection ……..…67

Chapter 5: Discussion……..……73

Bibliography……..….……..……...……79

List of tables

Table 1 Oligonucleotides used in generation of plasmids for expression of RRV vFLIP and truncated vFLIP proteins, and siRNA against vFLIP mRNA

Table 2 Oligonucleotide primers used in real time PCR

List of figures

Figure 1. Schematic comparison of selected open reading frames in three gamma herpesviruses

Figure 2. Construction of ORF71 expression plasmids

Figure 3. Schematic illustration of the truncations of ORF71

Figure 4. Subcellular localization of RRV vFLIP fusion with YFP

Figure 5. Detection of RRV vFLIP fusion proteins by Western blot analysis

Figure 6. Detection of PARP-1 and procaspase-9 by Western blot analysis

Figure 7. Activity assay of caspase-3, -7, -8, and -9

Figure 8. Detection of MnSOD transcript in cells with RRV vFLIP expression

Figure 9. Cell viability assay of HeLa cells after apoptosis induction

Figure 10. NF-κB reporter assay in HEK293 cells

Figure 11. Subcellular fractionation of HeLa cells to determine NF-κB nuclear translocation

Figure 12. Effect of RRV vFLIP on HeLa cells under starved condition

Figure 13. Increased autophagosome formation in HeLa cells after apoptosis induction

Figure 14. Upregulation of LC3-II in RRV vFLIP expressing cells after apoptosis induction detected by Western blot analysis

Figure 15. Effect of 3-MA treatment on anti-apoptotic function of RRV vFLIP

Figure 16. Effect of ammonium chloride treatment on anti-apoptotic function of RRV vFLIP

Figure 17. Autophagosome formation in HeLa cells after rapamycin induction

Figure 18. Inibition of rapamycin-induced autophagy in HeLa cells. Reduction of of LC3-II in RRV vFLIP-expressing cells after rapamycin induction.

Figure 19. Expression of the truncation variants of RRV vFLIP protein

Figure 20. Truncation variants of RRV vFLIP protein are unable to inhbit apoptosis

Figure 21. Truncation variants of RRV vFLIP protein are unable to inhbit rapamycin-induced autophagy

Figure 22. Latent infection of BJAB cells by RRV assists cell survival

Figure 23. Cell viability assay of BJAB and BJAB-RRV cells after apoptosis induction

Figure 24. siRNA-mediated suppression of vFLIP expression in HEK293 cells transiently transfected with VenusN1-vFLIP

Figure 25. siRNA-mediated suppression vFLIP expression in RRV-infected BJAB cells

Figure 26. Suppression of RRV vFLIP gene expression in BJAB-RRV cells leads to loss of anti-apoptosis function

List of abbreviations

3-MA	3-Methyladenine
aa	Amino acid
AP-1	Activator protein-1
APAF-1	Apoptotic protein activating factor
BCBL-1	Body cavity based lymphoma
BCL-2	B-cell lymphoma-2
BHV	Bovine Herpes virus
CAD	Caspase-activated deoxyribonuclease
CARD	Caspase recruitment domain
Caspase	Cysteinyl aspartate specific protease
cFLIP	cellular FLICE inhibitory protein
CHO	Chinese hamster ovary
CMV	Cytomegalo virus
CPE	Cytophathic effect
CTL	Cytotoxic T cell
DED	Death effector domain

DISC	Death inducing signaling complex
DMEM	Dulbecco's Modified Essential Medium
DNA	Deoxyribonucleic acid
EBV	Epstein-Barr virus
ELISA	Enzyme linked immunosorbant assay
FADD	Fas-associated protein with death domain
FBS	Fetal bovine serum
FITC	Fluorescein isothiocyante
FLICE	FADD-like interleukin-1 beta-converting enzyme
HBSS	Hank's balance salt solution
HEK 293	Human embryonic kidney 293
HHV	Human herpes virus
HPV	Human papilloma virus
HSV	Herpes simplex virus 1
hTERT	human telomerase reverse transcriptase
HVS	Herpesvirus saimiri
IAP	initiator of apoptotic protein

IFA	Immunofluoresecne assay
IKK	Inhibitor of Kappa B kinase
IκB	Inhibitor of Kappa B
kb	Kilo-bases
kDa	Kilo Dalton
KSHV	Kaposi's sarcoma-associated herpesvirus
LANA	Latency nuclear associated antigen
LC3	Microtubule associated light chain 3
LPD	lymphoproliferativ disorder
MCD	Multicentric castleman's disease
MCF-7	Michigan cancer foundation-7
MnSOD	Manganese superoxide dismutase
mTOR	mammalian target of rapamycin
NEPRC	Newengland primate research center
NF-κB	Nuclear Factor of Kappa B
NOD/SCID	Non-obese diabetic/Severe combined immunodeficiency
nt	Nucleotide

OMM	Outer membrane mitochondria
ORF	Open reading frame
PAA	Phosphonoacetic acid
PARP-1	Poly(ADP-ribose) polymerase-1
PBS	Phosphate-buffered saline
PCR	Polymerase chain reaction
PCR	Polymerase chain reaction
PEL	Primary effusion lymphoma
pRb	Retinoblastoma protein
RHF	Rhesus fibroblast
RRV	Rhesus rhadinovirus
RTA	Replication transcription activator
RT-PCR	Real-time polymerase chain reaction
SDS	Sodium dodecyl sulphate
SIV	Simian immune deficiency virus
SPF	Specific pathogen free
TNFR	Tumor necrosis factor receptor

TNF-α	Tumor necrosis factor-α
TRAIL	TNF-related apoptosis inducing ligand
TRAM	TNFR-related apoptosis mediating protein
TS	Thymidilate synthetase
vCyclin	viral Cyclin
VEGF	Vacular endothelial growth factor
vFLIP	viral FLICE inhibitory protein
vIL-6	viral interleukin-6
vIRF	viral interferon regulatory factor
VZV	Varicella zoster virus

Chapter 1: General introduction

1.1 Introduction

Herpesviridae is one of the large and extensively diverse families of DNA viruses. Due to its huge genomic capacity, herpesviruses encode many genes, which are responsible for a variety of biological functions during infection. *Herpesviridae* is divided into three major subfamilies, Alpha, Beta, and Gamma, on the basis of genomic organization, sequence relatedness, and biological properties (16). Herpesvirus is able to infect a wide range of hosts and has broad effects on several systems including urogenital tract, integument, immune and neurological system and so forth. A unique characteristic of herpesvirus infection is life-long latency after primary infection. Currently, there are eight human viruses that belong to *Herpesviridae*, HSV-1, HSV-2, VZV, EBV, CMV, HHV-6, HHV-7, and HHV-8 (107).

The three major subgroups of herpesviruses cause different pathologic diseases. Several of the gamma herpesviruses have cellular transformation and oncogenic properties. So far, the genomes of eight gamma herpesviruses have been sequenced and their genetic similarity and differences have been analyzed (5). Rhesus rhadino herpesvirus was firstly identified and isolated at New England Primate Research center in 1997(19). An outbreak was investigated in the affected monkeys having antibody against herpesvirus saimiri (HVS). A mysterious virus was isolated from peripheral blood mononuclear cells of suspected rhesus macaques. Sequence analysis of this virus indicated that its sequence and genomic organization were closely related to HHV-8. This virus was classified in rhadinovirus subgroup and named rhesus

monkey rhadinovirus isolate 26-95 (RRV 26-95) (19). RRV strain 17577 was independently isolated from bone marrow of an SIV-infected monkey with the presence of lymphoma (91). Phylogenetic profiling suggested that RRV 26-95 and 17577 are different isolates of the same virus (2, 90).

The long unique region of the RRV genome is approximately 130 kb in length and consists of 84 ORFs. The genomic sequence analysis indicated the similarity of ORFs to KSHV. Examples are ORF2 (interleukin-6), ORF8 (glycoprotein B), ORF9 (DNA polymerase), which are closely related to KSHV. Notably, viral interleukin-6 gene is uniquely present in RRV and KSHV. Not only is RRV's genome orientation entirely collinear with KSHV, RRV genes are also in corresponding locations with the same polarity as those in KSHV (2, 19, 90, 91).

Although RRV infection of peripheral blood mononuclear cells is latent, it lytically replicates with high virus titer in rhesus fibroblast cells (RhFs) without any chemical induction (19). The kinetics of RRV gene expression in infection are characterized into immediate early, early, and late classes. Several genes encoding protein homologous to cellular proteins such as vIL-6, are classified as early genes (25).

Two major hindrances to KSHV study are the lack of an efficient cell culture system and an appropriate animal model. Although lytic replication can be accomplished by chemical induction, the virus yield is still unsatisfied (87). Several groups have been attempting to establish animal models for KSHV; however, there is no ideal animal model that develops clinical presentation similarly observed in KSHV infection (24, 86, 87). In contrast, virus models have been established. Two bonafide

candidates were proposed to study KSHV pathogenesis. They are herpsevirus saimiri (HVS) and rhesus rhadinovirus. Whereas the genomic sequence of HVS also has high similarity to KSHV, the target cell of HVS is T cells instead of B cells and there is no clinical presentation relevant to KSHV infection (50, 53). On the other hand, RRV-infected rhesus macaques developed lymphoma similar to mulitcentric castleman's disease (MCD) and primary effusion lymphoma (PEL) associated with KSHV infection (64). Therefore, RRV has been proposed as a virus model for KSHV infection.

ORF71 of RRV encodes the viral Fas associated death-domain like interleukin-1 β converting enzyme (FLICE) inhibitory protein (vFLIP). RRV vFLIP has approximately by 40 percent similarity to KSHV vFLIP based on DNA sequence (75, 91). This gene has also been found in tumorigenic human molluscipoxiviruses and gamma herpesviruses, such as KSHV, EHV, and HVS. The vFLIP contains two death effector domains commonly shared among several viruses and cellular FLIP (101). It indicates that vFLIP has the ability to inhibit apoptosis. It interrupts the binding between caspase-8 and FADD, which prevents the recruitment of death-inducing singaling complex. This interruption inhibits the cleavage of procaspase-8 to become an active form, caspase-8, eventually blocking the activation of downstream pathways of apoptosis (8, 12, 72). The exemplified function of vFLIP has been shown in KSHV vFLIP. Besides anti-apoptotic function, it is able to enhance the translocation of NF-κB from cytoplasm to nucleus (11). This activation of NF-κB causes the up-regulation of genes involved in apoptosis, cell proliferation, and inflammation that participates in tumorigenesis of KSHV (88, 99, 100). A recent study has shown that

KSHV vFLIP also suppresses autophagy, also known as type II cell death, by preventing Atg3 from binding and processing LC3 (58).

KSHV and RRV latent infections have been implicated in malignancies. Among the latent genes are ORF71, 72, and 73. Transcripts of vIL-6 and these three latent genes have been detected in lymphoma lesion from rhesus macaque, but the protein vFLIP was not detected. The detection of vIL-6 and vFLIP transcripts in the lesion from affected rhesus macaque suggested that expression of these two genes associates with B cell proliferative diseases and lymphadenopathy (76). In KSHV, the functions of viral genes, particularly vFLIP, expressed during latency have been well elucidated. Whereas several lines of evidence imply the association of RRV vFLIP in malignancy pathogenesis, functional characterization of this protein has not been reported to date.

1.2 Research objectives

Following are the specific objectives of the present study on RRV vFLIP

Objective 1: To determine the function of RRV vFLIP on apoptosis and NF-κB pathways

Objective 2: To assess the function of RRV vLFIP on autophagy pathway

Objective 3: To determine the function of vFLIP in BJAB cells latently infected with RRV

Chapter 2: Literature review

2.1 *Evolutionary and historical perspective of rhesus monkey rhadinovirus*

2.2 *Biology of rhesus rhadinovirus*

2.3 *Viral FLICE inhibitory protein of rhesus rhadinovirus*

2.4 *Apoptosis pathway*

2.5 *Autophagy pathway*

2.1 Evolutionary and historical perspective of rhesus monkey rhadinovirus

Herpesviruses belong to a large, linear, double-stranded DNA virus family. Most of herpesviral genomes contain many ORFs ranging from 70 to 120, with an exception of human cytomegalovirus (HCMV), which codes about 220 ORFs. The genome is contained within an icosahedral capsid, which is coated by a proteinaceous matrix and then wrapped in a lipid envelope. The members of Herpesviridae have been classified into three subfamilies: *Alphaherpesviriae*, *Betaherpesvirinae*, and *Gammaherpesvirinae*. Although *Herpesviridae* composes of a broad range of viruses, their genomes also share some conserved genes, such as DNA polymerase and glycoprotein B, across the species. The similarity can be determined from amino acid identity comparisons (16, 31, 73). There are eight known human herpesviruses. These include human herpes simplex 1 (HSV-1), Herpes simplex 2 (HSV-2), varicella-zoster virus (VZV), Epstein-Barr virus (EBV), cytomegalovirus (CMV), herpesvirus 6 (HHV-6), herpesvirus 7 (HHV-7), and herpesvirus 8 (HHV-8) or Kaposi's sarcoma associated herpesvirus (KSHV) (107).

Several gammaherpesviruses are potentially linked to oncogenic characteristics and cell transformation. EBV and KSHV are two bonafide examples involving in the pathogenesis of human cancers. EBV is highly associated with Burkitt's lymphoma, Hodgkin's lymphoma, and nasopharyngeal carcioma, and KSHV is a causative agent of Kaposi's sarcoma, primary effusion lymphoma (PEL), and multicentric Castleman's disease (MCD) (68, 114). Based on cellular tropism, two groups have been categorized: lymphotropism and T-cell tropism. Lymphocryptoviruses (B-cell-tropic) infect great apes and Old World primates. T-cell-tropic herpesvirus saimiri of New World primates and related members from horses, cattle, and other species are named as rhadinoherpesvirus (54).

In 1997, a herpesvirus related to KSHV was first identified from the colonies of rhesus monkey at New England Regional Primate Research Center. Serum samples from a large number of rhesus monkeys including healthy and affected animals contained antibodies against *Saimirriine herpesvirus 2* (Herpesvirus saimiri, HVS). The suspiciously related macaque virus was later isolated from peripheral blood mononuclear cells cocultured with rhesus monkey fibroblasts. CPE was observed on day 8 to 11 after the co-culture. The cells were completely destroyedby day 13 to 16. At low multiplicity of infection, foci were found in early destruction of monolayer cells, and became rounded and syncitial after infection spread. In addition, intranuclear inclusion bodies were visible in the regions where CPE was localized. Electron micrographs indicate that a number of viral particles were visible in the nucleus, cytoplasm, and extracellular space. Based on genomic organization, sequence relatedness, and predicted amino acid sequence, RRV isolate 26-95 was found to be highly closed to KSHV than HVS and any other

rhadinoviruses (19). In 1999, the rhesus rhadinovirus 17577 (RRV 17577) was independently isolated from bone marrow obtained from an SIV-infected juvenile rhesus macaque monkey with a lymophoproliferative disorder (PCD) (91). Its complete genomic sequence is greater than 99% identical at the DNA level with the RRV 26-95 isolate. From the genomic organization, ORF structure, and phylogenetic analysis similarity, it was suggested that the RRV 26-95 and RRV 17577 are different isolates of the same virus (90).

2.2 Biology of rhesus rhadinovirus

Genome structure and organization

The first partially sequenced genome of RRV 26-95 was obtained in 1997. Column-purified virions without any restriction endonuclease digestion provided DNA of more than 25 kbp in length on agarose gel electrophoresis. After digestion with *Pst*I, *Hind*III, and other restriction endonucleases, a broad range of genetic fragments in different sizes were observed (19). The complete sequencing of two *Pst*I clones yielded 10595 bp of partial genome containing the DNA polymerase and glycoprotein B genes. Interestingly, the BLAST search analysis of the 10595 bp showed that ORF8 (intact gene for glycoprotein B), ORF9 (DNA polymerase), ORF10, 11, and ORF R2 (viral interleukin-6) and pertain gene for thymidilate synthetase (TS, ORF70) represented the highest levels of similarity to KSHV, herpesvirus saimiri, and other rhadinoviruses (19, 91). The predicted amino acid sequences over this region, which contains ORFs 8, 9, 10, 11 and R2,, were slightly closer to KSHV than other herpesviruses. The selected region for sequencing not only provided information related to conserved gene block (DNA

polymerase and glycoprotein B genes), but also conferred the variation in nonconserved region (R2) among other rhadinoviruses. The new viral genome contains the viral interleukin-6 (vIL-6) gene, which is not present in HVS and any other herpesviruses. TS gene promptly comes after vIL-6 in the new virus, while in KSHV, dihydrofolate reductase (DHFR) and K3 genes are intercalated between vIL-6 and TS. Although DHFR and TS genes have been identified in KSHV and HVS, they are not found in other herpesviruses. The location of DHFR and TS genes in HVS genome is different from KSHV. Based on these similarities in genome organization and sequences, this new virus was classified to the rhadinovirus subgroup and named rhesus monkey rhadinovirus (RRV). In 1999, Robert and his colleagues independently isolated rhesus rhadinovirus (RRV) strain 17577 from a simian immunodeficiency virus (SIV)-infected macaque with lymphoproliferative disorder (LPD), of which lesion was similarly observed in MCD patients. The full length of the viral genome was successfully sequenced and characterized. The entire long unique region (LUR) of the genome of an RRV strain 17577 contains 131364 bp in length and consists of 79 ORFs, of which 67 ORFs corresponding to ORFs of KSHV and HVS. In RRV isolate 26-95, its L-DNA has 130,733 bp that contains 84 ORFs and 83 of them correspond to ORFs in RRV 17577. Only one ORF, which belongs to RRV 26-95, but not RRV 17577, contains the sequence of herpesvirus core gene ORF 67.5. Although the genome organization of RRV isolate 26-75 is not entirely co-linear with that of KSHV, in most cases, its genes are in corresponding locations and same polarity as KSHV genes (90).

Some ORFs are uniquely present in KSHV, but not in RRV 26-75. These include K3 (bovine herpesvirus-4 immediately-early protein homologous), K7 (nut-1), and K12

(kaposin). The sequence differences between KSHV and RRV suggest that these KSHV-specific genes were acquired subsequent to the divergence of Asian and African Old World primates (73). Some sets of genes are partially shared between KSHV and RRV. For example, RRV 26-95 contains only one vMIP-1 homologue, while KSHV has three, and RRV 26-95 contains eight homologues of vIRF, while KSHV has four.. In addition, an ORF encoding 102-aa polypeptide was found in RRV genome and corresponds in location to K4.1, K4.2, K5, K6, and K7 of KSHV. In conclusion, RRV26-95 is closely related to KSHV in sequence and genome organization (90).

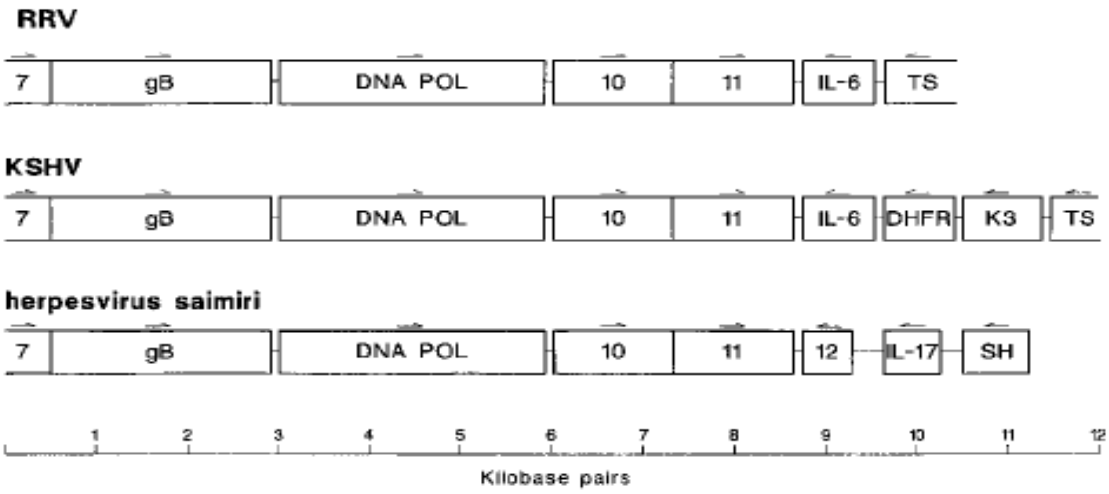

Figure 1. Schematic comparison of selected open reading frames in three gamma herpesviruses: RRV, KSHV, and HVS. (19)

Viral attachment and entry

Herpesviruses employ the engagement of multiple receptors to infect a broad range of hosts. The binding of host receptors by viral glycoproteins is the first step for viral entry. Viral DNA is encapsidated in icosahedral structure, which is coated with a

layer of protein called the tegument. The outside surface is enveloped with viral proteins and glycoproteins incorporated in a lipid bilayer. It has been well studied that glycoproteins are greatly essential for the virus entry. Several glycoproteins on virion envelope have been identified in the herpesvirus family such as glycoprotein gB, gC, gD, gH, gL, gp42, gp350, HHV-8 K8.1A, and so forth. At least three glycoproteins have been suggested to participate in the entry of all herpesviruses including glycoprotein B, glycoprotein H, and glycoprotein L. The genes of these glycoproteins are conserved among herpesvirus family. The highest degree of similarity is exhibited in glycoprotein B. The glycoprotein B can be either homodimer or herterodimer with gH and gL to form a prominent spike (97).

Most herpesviruses gain entry into cells through the initial interaction with the cell surface glycosaminoglycans, usually heparin sulfate, but a notable exception is EBV (94). So far, three classes of herpesvirus entry receptors have been described. These include herpesvirus entry mediator (HVEM, a member of the tumor necrosis factor receptor family); nectin (a member of the immunoglobulin superfamily); and 3-O-sulfotransferases (an enzyme to catalyze the transfer of sulfate to heparin sulfate) (96). Different viral glycoproteins have the ability to bind different types of host receptors. For example, herpesvirus gC and HHV-8 K8.1A are able to specifically bind heparin sulfate and EBV gp350 targets CD21 (B cell receptor), while HSV gD is able to interact with several cell surface receptors including HVEM, nectins, and 3-O-sufated heparan sulfate (37, 40, 93). The fusion of viral envelope with the plasma membrane of host cells is an important step for successful infection. An experiment investigating the viral entry by using CHO cells showed that the cells expressing the HSV glycoproteins including gB,

gD, gH and gL were able to fuse with other CHO cells expressing cellular receptors. The fusion of cells was determined by quantifying expression of a reporter gene activated only in heterokaryons. The underlying mechanisms on how HSV gD interacts with host cell receptors and facilitates viral entry or cell fusion remain unclear. However, it has been suggested that the conformational change during the binding of gD to one of its receptors enable the interaction between gD and gB or gH-L to enhance fusion activity (70). Most herpesviruses gain entry into a cell by either plasma membrane fusion or endocytosis. Plasma membrane fusion is a simple pathway, in which optimal pH between cell membrane and viral envelope is not essential for gaining entry (84). In endocytosis pathway, however, low pH at the fusion between the membrane of internalized vesicle and viral envelop is very critical in facilitating the release of viral nucleocapsid into cytoplasm. Then, the viral genome will be delivered into the nucleus through nucleocapsid trafficking (95).

Based on the nature and size of cargo in endocytosis, the entry has been classified into clathrin-mediated endocytosis, caveola-mediated endocytosis, clathrin- and caveola-independent endocytosis, and macropinocytosis (71). The most commonly observed uptake pathway for viruses is the clathrin-mediated pathway. Clathrin-coated subunits have to detach from the surface of clathrin-coated vesicles containing virus before it fuses with early endosome. The viral particle then fuses with endosome and delivers its capsid to cytosol. Several observations showed that KSHV, RRV, and other herpesviruses utilize clathrin-mediated endocytosis for viral internalization (117).

Cell types supporting RRV replication

RRV infects a broad range of cell types. In natural infection, the virus can be found in peripheral blood mononuclear cells (PBMCs). B lymphocytes, a subset of PBMCs, have been shown to harbor RRV in latency phase (7). The study of molecular virology regarding viral entry, gene expression, and DNA replication requires cell lines that support efficient replication of virus. Although RRV latently infects PBMCs in rhesus macaques, it is able to lytically replicate in fibroblast cells. In a previous study, rhesus monkey fibroblast cells derived from skin punch biopsy were first described to coculture with PBMCs from a monkey infected with RRV (19). Several efforts were made to increase the lifespan of primary cell lines due to the limitation of a maximum passage of 38 for wild type rhesus fibroblasts. An early strategy was to introduce oncogenes E6 and E7 of human papilloma virus (HPV) in order to establish immortalized primary cell lines (14). However, the two proteins introduced to cells interfere with cellular process by degrading p53 and retinoblastoma tumor suppressor protein (pRb) (106). Thus, it is difficult to evaluate the effect of viral gene expression on cell cycle, or cell signaling. In addition, phenotypic changes and aberrations in growth characteristics are observed as well. Another strategy is to introduce the gene encoding telomerase, an enzyme that elongates telomere, into the cells. To establish an immortalized cell line that supports RRV infection, Krichchoff and colleagues employed a recombinant retrovirus technology to introduce the gene encoding catalytic subunit of telomerase (hTERT) into rhesus fibroblast cells (Telo-RhF) (46). These cells can be used for the study of viral gene expression, lytic replication, and transcription mapping. This cell line provides the similar growth pattern as normal RhFs and telomerase does not affect viral replication.

Viral gene transcription and expression

The hallmark of virus life cycle commonly shared among the herpesvirus family is the establishment of lytic and latent infection.

Unlike KSHV and EBV, RRV can efficiently replicate without any chemical induction in permissive cell lines like rhesus fibroblast (RhFs). The kinetic of gene expression in RRV following the de novo infection of rhesus fibroblasts was classified into immediate early, early, and late class (25). In immediate-early class, RRV ORF50 gene was transcribed between 6 and 12 h post-infection (hpi). The transcript of ORF50 gene (approximately 4 to 5 kb) is spliced into two new transcripts. These transcripts were named R8 and R8.1 due to homology to KSHV K8 and K8.1 respectively. However, the transcription of ORF50 is sensitive to cycloheximide (an inhibitor of protein synthesis) treatment, while phosphonoacetic acid (PAA, an inhibitor of DNA polymerase) fails to inhibit its expression. ORF57 is an immediate-early gene that has been described as post-transcriptional regulator. Its function has been suggested to be responsible for an increase of ORF50 transcription at an early time point. It was first detected at 6 hpi before the presence of RRV ORF50 and not inhibited by cycloheximide. It suggests that ORF57 reactivates the viral lytic cycle in conjunction with ORF50 or the ORF50 expression is undetectable at early time point due to its low abundance. In early class, R1 gene first appeared between 12 to 24 hpi. Its roles in lymphocyte signaling and cell transformation were characterized (21). Several of early class genes encode proteins homologous to cellular proteins, such as vIL-6. The activity of RRV vIL-6 has been demonstrated in cell culture system, and is most likely to have the same characteristic as KSHV vIL-6. The initiation of RRV vIL-6 gene expression is detected between 12 and 24 hpi. Inhibition of

vIL-6 gene expression caused by cycloheximide was observed at 12 and 20 hpi, while PAA did not affect its expression. Latency-associated nuclear antigen (LANA) is encoded by ORF73 that is present in both KSHV and RRV. Functions of KSHV LANA have been well elucidated, while RRV LANA remains unclear. LANA has a number of functions in the viral life cycle, including establishing latency in KSHV infection by tethering viral episome to chromosome during cell division. In RRV, however, LANA gene transcription was sensitive to cyctoheximide and PAA. In addition, vFLIP and vCyclin genes, classified as latent genes, had very similar patterns to that observed in KSHV vFLIP and vCyclin genes. It might be possible that ORF71, 72, and 73 have a bicistronic or tricistronic transcription pattern. The transcripts of vCyclin and vFLIP genes first appeared at 12 hpi and were sensitive to cycloheximide, but sensitive to PAA treatment at 30, 36, and 40 hpi. The upregulation feature of latent gene transcripts including RRV LANA, vFLIP and vCyclin during de novo infection of rhesus fibroblasts was different from the kinetic of gene expression in B cells latently infected with KSHV. In late class transcripts, ORF62 was first detected at 24 hpi. Its transcription was abolished to PAA and cycloheximide treatment at 12 hpi. The function of ORF62 product in RRV is unknown. However, based on homology to other herpesviruses, it was implied to play a role in viral assembly and DNA maturation. Recently, crystal structure of KSHV ORF62 product suggested that it is a member of triplex in viral capsid. In addition, RRV vIRF and gB genes, encoding viral interferon regulatory factors and viral glycoprotein B, respectively, have also described as late genes (20, 22, 25).

Rhesus rhadinovirus: pathogenesis and animal model system for KSHV

A major hindrance for KSHV study is the lack of an *in vitro* system for elucidation of its lytic replication. Although KSHV can infect a wide variety of primary cells and cell lines to a certain degree, none of them supports the replication of virus for high titer production. While chemical reagents like phorphol ester are used to induce lytic replication *in vitro,* their application for *in vivo* setting is limited (87). Many *in vitro* experiments and transgenic animal models have been developed to elucidate the pathogenesis of KSHV infection. Recently, Dittmer and colleagues employed SCID-human Thy/Live mice reconstituted with the liver and thymus of human fetuses to investigate the viral transcription and susceptibility of the mice to infection with KSHV derived from BCBL-1 cells (86). Furthermore, NOD/SCID mice were utilized to study lytic and latent viral gene expression and cell tropism (77). Whereas the previous studies have demonstrated the KSHV infection of transgenic mice, none of these models is able to elucidate the cellular activation in KSHV-associated diseases and virus-host interactions in latent infection. More recently, Chang and colleagues have demonstrated that KSHV infects a New World primate, common marmosets (*Callithrix jacchus, Cj*). They have shown that rapid seroconversion and high antibody responses for over one and a half years were observed in common marmosets intravenously inoculated with recombinant KSHV. Furthermore, KSHV DNA and LANA protein were present in PBMCs and tissues of infected marmosets. Surprisingly, two marmosets orally infected with rKSHV.219 developed a KS-like lesion with characteristic spindle cells along with small blood vessel and extravasated erythrocytes, which were similar to human KS lesion in histopathological features. However, the prevalence of LANA-positive staining in KS-

like lesion in the marmosets was not as strong or widespread as those of human KS lesions. In addition, only two KSHV-infected marmosets developed KS-like lesions, which were not statistically significant for a conclusion of KS-like lesion development after KSHV infection (10).

Several groups have been exploring related viruses as models for KSHV. Two examples of this model are HVS and RRV, which have genomic organization and sequences closely related to KSHV. In New World primates infected by HVS, animals develop an aggressive, fulminant lymphoma, which is related to MCD and PEL. But the target cells are T lymphocytes instead of B lymphocytes found in KSHV and RRV infection (50, 53, 54). An early study showed that SIV-infected rhesus macaques inoculated with RRV developed B-cell LPD. Two clinical presentations including persistent angiofollicular lymphadenophaty, closely relate to MCD and hypergammagloubulinemia that are usually observed in AIDS patients coinfected with KSHV. A recent paper reported that rhesus macaques coinfected with SIV and RRV had B cell hyperplasia. However, abnormal cellular proliferation as B-cell lymphoma and a proliferative mesenchymal lesion was observed at a low percentage of these animals (112). More recently, Orzechowska and colleagues (76) reported the involvement of RRV in non-Hodgkin's lymphoma--a diverse group of blood cancers that include all kinds of lymphomas except Hodgkin's lymphoma. Rhesus macaques were intravenously infected with SIVmac239 to induce immunodeficient condition, and at 8 weeks after SIV infection, inoculated with RRV 17577. The monkeys developed latent and persistent RRV infection, lymphoma and retroperitoneal fibromatosis. Analysis of viral gene expression associated with the development of lymphomas was performed. The transcripts encoding RRV ORF-R2

(vIL-6) and ORF71 (vFLIP) were detected, which is consistent to a previous report on vIL-6 in KSHV-infected PEL cells (110). Whereas RRV infection in rhesus macaques presents clinical features similar to KSHV-associated MCD and PEL, no evidence of clinical presentations similar to Kaposi's sarcoma has beenfound. Therefore, an alternative model to study the pathogenesis and disease progression of Kaposi's sarcoma still needs to be developed.

Epidemiology

To detect antibody against RRV, an ELISA test was developed by coating the plate with purified RRV 26-95 virions. The prevalence of RRV infection was tested from serum samples of 56 randomly selected rhesus macaques, which were from specific-pathogen-free (SPF) colonies at the New England Regional Primate Research Center (NERPRC). Fifty-two of the 56 SPF monkeys (92.8%) were strongly positive for the presence of antibody against RRV strain 26-95. In addition, serum samples of many monkeys from a conventional colony at NERPRC also had highly reactive antibodies against this virus. The high rate of antibody detection suggested a high prevalence of RRV infection in the colony. Interestingly, serum samples taken from rhesus monkeys at NERPRC in 1985 and stored frozen also showed a high rate of strong antibody reaction. In addition, serum samples from rhesus monkeys at two other institutions were also tested. All of forty serum samples from one primate facility and a commercial supplier showed strong antibody reaction against RRV. Several lines of evidence demonstrated that rhesus monkeys were naturally infected with a herpesvirus in the rhadinovirus subgroup. The route of natural infection remains unclear, but evidence from KSHV and observation from high rate of seropositivity implied that the oral route may be a major

route of transmission. It was reported that close contact might be required for infection by other gamma herpesviruses (15, 19).

Diagnosis

Many diagnostic tools are available to investigate RRV infection. One of the most sensitive and less time-consuming methods is to detect the presence of antibody in serum. Whole-virus ELISA was developed and used to determine RRV serological status of monkeys in a colony (19). Serum samples from monkeys 4 to 7 months after birth were negative for the presence of antibody. However, subsequent serum samples from these monkeys after 1 year became strongly positive.

Viral isolation and PCR are also employed for RRV diagnosis. Viruses isolated from peripheral blood mononuclear cells are able to infect primary fibroblast cells and cause efficiently lytic infection. High viral yield can be further determined with other methods. In addition, plasma, whole blood, and other biological specimens are the source for DNA isolation and amplification by using PCR. Although detection of nucleic acid with PCR can provide beneficial information for diagnosis, it requires caution to interpret negative results due to less sensitivity than serological assays (64).

2.3 Viral FLICE inhibitory protein

vFLIP in human molluscipoxviruses and several herpesviruses including KSHV, EHV-2, and HVS was found to inhibit apoptosis induced by death receptors (101). Interaction between extracellular death stimuli and death receptors causes the recruitment of the adapter molecule Fas-associated death domain (FADD), which interacts with procaspase-8 to form a complex, known as the death-inducing signaling complex (DISC).

The DISC formation allows procaspase-8 to be cleaved into its active caspase-8 and subsequently activates other downstream effector caspases, leading to apoptosis. The recruitment of DISC relies on interaction between death effector domains that present in adaptor protein like FADD and N-terminus of procaspase-8 (12, 72). Several viruses targeting apoptosis pathway employ different strategies to block Fas and tumor necrosis factor receptor (TNFR) signaling. For example, the E3-10.4 protein of adenovirus is able to degrade Fas (23). M-T2 protein secreted from myxoma virus can bind to TNF and interfere with its binding to TNFR. Four different proteins (crmB, C, D, and E) encoded by cowpox virus are able to inhibit TNF activity. Some viruses suppress apoptosis by inhibiting the activity of caspases. Adenovirus 17.4 protein and crm A inhibit activity of caspase-8 and inhibitor of apoptosis protein (IAP) (39). Many of gamma herpesviruses employ vFLIP to interfere with interaction between caspase-8 and FADD. vFLIP contains two death effector domains (DEDs) that has been shown to bind to DEDs of FADD and capase-8. In addition, EHV-2 E8 gene encoding a DED-containing protein was demonstrated to block the recruitment of DISC (6). Raji B cells expressing vFLIP are resistant to apoptosis (36). Furthermore, the other receptors that belong to death receptor subfamily or TNFR such as TNFR-related apoptosis mediating protein (TRAMP) and TNF-related apoptosis-inducing ligand (TRAIL) were also blocked by coexpression of vFLIP. Similarly, Cellular FLIP or cFLIP also is also involved in the inhibition of apoptosis pathway via the activation of several death receptors including CD95, TNFR 1, TRAIL1 and 2, and TRAMP (39).

Structure and function of two death effector domains of vFLIP

The structure of vFLIP consists of six antiparallel α-helices, which are commonly shared by caspase recruitment domain (CARD). Although two DEDs were similarly observed in FADD, vFLIP, cFLIP, and caspase-8, different residues in DEDs make their individual structures unique (33). Whereas DED-containing proteins have been known to inhibit apoptosis, the underlying mechanisms are still unclear. The structure of the tandem DEDs of MC159 was first crystallized(61). The full-length protein consists of two tandem DEDs and a C-terminal extension. DED1 and DED2 are bridged by a stretch of 14 amino acids, which form a short helix α7 and two surface loops. Both structure and sequence anaylsis suggested that the interaction at the DED1 and DED2 interface are highly conserved among all proteins that contain tandem DED domains. This conserved rigid structure and interface between the tandem DEDs can be an ideal model of vFLIPs, c-FLIP, caspase-8, and caspase-10. Although there is no sequence homology between DEDs of MC159 and CARD domains of apoptotic protease activating factor 1 (Apaf) and caspase-9, the interaction between two DEDs is similar to that between the CARD domains (82). The interaction between caspase-8 and vFLIP are thought to antagonize apoptosis. MC159 employs two conserved surface binding elements to interact with the DEDs of caspasea-8.

vFLIP was encoded by several viruses including KSHV, RRV, HVS, EHV, bovine herpesvirus (BHV), molluscum contagiosum virus (MCV), and Sindbis virus (SV), (101). Although they share common structure, vFLIPs from different viruses function differently. Functional characterization of KSHV vFLIP has been more extensively investigated than the other herpesviruses. KSHV vFLIP inhibits caspase-8

acitvation. Comparative proteome analysis showed that manganese superoxide dismutase (MnSOD), a mitochondrial antioxidant and an important antiapoptotic enzyme, was dramatically upregulated in endothelial cells expressing KSHV vFLIP (103). A unique feature of KSHV vFLIP distinct from other vFLIPs is that it constitutively activates NF-κB pathway through enhancing the degradation of IκB, which allow RelA/p65 subunits to translocate into the nucleus and activate gene transcriptions (11, 30). The activation of NF-κB pathway is very important in at least two aspects: maintenance of latent infection and transformation. NF-κB activation can greatly suppress the AP-1 pathway, which is essential for lytic replication. In terms of oncogenesis, KSHV vFLIP can transform Rat-1 cells by activation of NK-κB signaling. This finding was substantiated by observation of tumor development in nude mice injected with Rat-1 cells expressing KSHV vFLIP (100). Furthermore, NF-κB activation is able to prevent anoikis, a type of programmed cell death in anchorage-dependent cells detaching from the surrounding extracellular matrix. It was suggested that anoikis is inhibited by vFLIP through inducing the secretion of some paracrine survival factors. vFLIP inhibition, however, does not protect cells from apoptosis induced by the removal of essential survival factors, including vascular endothelial growth factor (VEGF) (26). Recently, Lee and colleagues (58) found another role of KSHV vFLIP on autophagy, a type II programmed cell death with accumulation of autophagosomes. The viral and cellular FLIPs suppress rapamycin-induced autophagic cell death by preventing Atg3, a protein enhancing autophagosome formation, from binding and processing LC3, an important protein residing in autophagosomes.

RRV vFLIP

Like other gamma herpesviruses, RRV also encodes vFLIP. Based upon the primary DNA sequence of RRV 26-95, ORF71, which encodes vFLIP, has 40.1% and 99.4% similarity to KSHV and RRV isolate 17577, respectively (75). RRV vFLIP is also expressed during latency period as observed in other herpesviruses. Although RRV has been proposed to be a model to study the KSHV pathogenesis, the functions of several latent genes such as LANA, vCyclin, and vFLIP are still unclear. However, an experiment in rhesus macaques suggested that vIL-6 and vFLIP involve in the RRV pathogenesis in B cell hyperplasia and persistent angiofollicular lymphadenopathy, which resembles to MCD associated with KSHV (110). Transcripts of RRV ORF-R2 and ORF71, which encodes vIL-6 and vFLIP, respectively, were detected in the lymphoma tissues from rhesus monkeys coinfected with RRV and SIV. So far, functional characterization of RRV vFLIP has not been reported.

2.4 Apoptosis pathway

Apoptosis, a programmed cell death, plays a key role in multicellular organism to get rid of unwanted cells. The term “apoptosis” was coined by Currie and colleagues in 1972 to characterize a common type of programmed cell death in various cell types. Under microscopic observation, these dying cells shared the morphologic changes, which were different from the features in necrotic cell death. It was suggested that these features might result from the underlying conserved biochemical events. During early apoptosis, most organelles in the cytoplasm, except mitochondria and Golgi apparatus, are packed tightly and chromatin in the nucleus starts condensing irreversibly. In the late state, the

entire cell is associated with cell shrinkage and membrane blebbing in order to reorganize a number of small seal membranes that are often referred to as “apoptotic bodies”. The size of these membrane-bound vesicles can vary from 0.5 to 2 μM. They also contain the various combinations such as part of condensed nuclei or organelles and cytosolic elements (45). These bodies are subsequently engulfed and digested by other cells such as macrophages and parenchymal cells. In this process, no inflammatory reaction is detected due to the following reasons. First, the cells that die via apoptosis do not release any of harmful cellular constituents such as hydrolase, protease, and lysozyme into the interstitial space. Second, this complicated mechanism does not promote the secretion of pro-inflammatory cytokines. Last, the rapid phagocytosis by surrounding cells can prevent secondary necrosis (89). The morphological changes during apoptosis get involved in highly complicated biochemical events and are energy dependent. Two important players in apoptosis are evolutionarily conserved protein families, namely the BCL-2 family of apoptosis regulatory proteins and the Cysteinyl Aspartate-Specific proteASE (Caspase).

BCL-2 (B-cell lymphoma) protein family was discovered in chromosomal translocation involvingchromosome 14 to 18 in B-cell follicular lymphoma. It triggers the excessive driving of immunoglobulin heavy chain gene promoter and enhancer on chromosome 14 (13). BCL-2 plays a role in promoting cell proliferation and inhibiting cell death (105). The functions of BCL-2 are essentially diversified in apoptosis, development, programmed cell death, tissue turnover, and host defense against pathogens (60). So far, at least 12 core BCL-2 family proteins have been identified in mammals. These include the BCL-2 itself and the proteins that share the three dimensional structure

or predicted secondary structure with BCL-2. The unique feature of BCL-2 protein family is that they contain the so called BCL-2 homology domains (BH1, BH2, BH3, and BH4). BH3-containing proteins, the most common in the family, are related to promote apoptosis through the regulation and interaction with the other core BCL-2 family proteins. In mammals, the members of BCL-2 protein family are classified into three subfamilies: BCL-2 subfamily (pro-survival), Bax subfamily (pro-apoptotic), BH3 subfamily (pro-apoptotic). BCL-2 subfamily consists of several members such as BCL-2, BCL-XL, BCL-W, MCL1, BCL-B and A1 (44). Their major function is to inhibit apoptosis. The deletion of genes in the BCL-2 subfamily leads to arrays of cell defects. Knockout BCL-2 gene causes abnormal death of renal epithelial progenitor (29). Abnormal death of fetal erythroid progenitor and neurons was promoted by deletion of BCL-XL gene (105). The absence of BCL-W gene resulted in abnormally accelerated death of granulocytes and mast cells (80). BCL-2 and BCL-XL have anti-apoptotic function via binding and regulating Bax subfamily proteins (BAX and BAK). BAX/BAK activation is a critical step to induce cells to undergo apoptosis through inducing permeabilization of the outer mitochondrial membrane (OMM) and the subsequent release of cytochrome C, which further trigger caspase-9 activation and execution (43). The members of BH3 subfamily such as BAD, BIK, BID, BIM, NOXA, and PUMA contain a conserved BH3 domain that allows them to interact with anti-apoptotic BCL-2 proteins to promote apoptosis. The deletion of genes in BH3 subfamily can cause several defects. For example, BID-deficient mice are resistant to Fas-acitvation-induced hepatocyte killing and fatal hepatitis. Cells with depletion of PUMA gene are resistant to DNA damage. Lacking of BAD in some cell types leads to mild resistance to deprivation

of epidermal or insulin growth factors. And lacking of BIM leads to abnormal accumulation of lymphoid and myeloid cells (98).

Caspases

Caspases are cysteine proteases that can cleave substrates after an aspartate residue at sites bearing tetrapeptide motifs. Caspase-1 (interleukin-1β-converting enzyme or ICE) was the first identified caspase in humans. In *Caenorhabditis elegans**, ced-3*** gene **(**cell-death abnormality-3) was discovered to encode a cysteine protease closely related to the mammalian ICE (116). At least 14 caspases have been identified in mammals, of which 11 have been found in humans. Furthermore, the homologues of caspases have been reported in several species, such as *Drosophila melanogaster* (common fruit fly), *Spodopteran frugiperla* (fall army worm), and *Saccaromyces cerevisiae* (yeast). The crystal structures of caspases including mammalian caspase-1, -2, -3, -7, -8, -9 and *Spodopteran frugiperla* caspase-1 have been well studied (55). The highly conserved caspase monomer consists of two subunits; one large and one small. Homodimerization of several monomers leads to the conformational structure of the active site. Caspase activation pathway is commonly conserved among nematodes, fruit flies, and mammals. The function of caspases involves several cellular pathways including apoptosis, inflammatory response, and necrosis (56). However, at least 7 out of 14 known mammalian caspases play key roles in apoptosis. There are two classes of apoptotic caspases; initiator and effector. Newly synthesized caspases in cells do not function and must be proteolytically activated during apoptosis signaling. Activation of an effector caspase requires cleavage by an initiator caspase at specific internal aspartic acid residues. In contrast, the initiator caspases can autolytically activate themselves and

trigger a cascade of downstream activation. Once effector caspases are activated, the proteolytic cleavage of a broad spectrum of cellular targets triggers apoptosis (28).

Intrinsic pathway

The intrinsic pathway requires no extracellular receptor to trigger apoptosis, but the intracellular signals take part in apoptosis. The stimuli could act in either negative or positive manner depending on interaction of either pro-apoptotic or anti-apoptotic cellular proteins. The disruption of mitochondria membrane and the release of cytochrome C into cytosol enhance the activity of cytosolic protein called Apaf-1, which recruit procaspase 9 to assembleapoptosome, a caspase-activating complex. This results in an activation of caspase-9 and initiation of the execution caspase pathway.

Extrinsic pathway

Extrinsic pathway is initiated from the interaction between ligands and receptors at the transmembrane. Ligands can be either soluble factors or receptors that are present at the surface of the cells such as cytotoxic T lymphocytes (CTL). TNF-family ligands exert their biological functions within the immune system, inflammatory responses, and apoptosis. Death receptors on cell surface belong to the tumor necrosis factor gene superfamily (TNF). The members of TNF receptor family contain the cysteine-rich repeats of 40 amino acids at extracelluar amino acid terminal. Some also share the similar sequence in cytoplasmic regions, while others contain homologous region in intracellular domains known as death domains. The binding of death-inducing ligands and TNF superfamily receptor initiates the fusion of lipid raft, which leads to the clustering of extracellular death receptors and conformational change in the intracellular domains. A

variety of apoptotic proteins are then recruited to form protein complex, Death Inducing Signaling Complex (DISC), followed by the activation of caspase-8 and effector caspases in the execution pathway.

Execution pathway

Execution pathway is considered as the final part of apoptosis, where intrinsic and extrinsic pathways eventually merge at this point. Caspase-3, -6, and -7 act as effector molecules to induce degradation of nuclear materials by activation of cytoplasmic endonucleases. Caspase-3 is considered as the most important executioner because it receives signal from both extrinsic and intrinsic pathways through caspase-8 and -9, respectively. Finally, caspase-3 enhances the release of caspase-activated deoxyribonuclease (CAD) from its inhibitor to degrade chromosomal DNA.

Perforin/granzyme pathway

Perforin and granzyme are granules in cytotoxic T lymphocytes (CTLs). They are released after CTLs bind to target cell receptor such as FasL/FasR. During degranulation, perforin inserts into the plasma membrane, forms a pore, and allows the granzyme to get into the pore. Granzyme, a serine protease, has been characterized into two major types; A and B. Granzyme B promotes apoptosis by activating procaspase-10 and cleaving inhibitor from CAD, while Granzyme A induces apoptosis via a caspase-independent pathway.

2.5 Autophagy

Autophagy was first introduced at the CIBA Foundation Symposium on lysosomes in 1963 by Christian de Duve, who is considered as the founding father of this research area (47). The term autophagy (from “auto” oneself, “phagy” to eat) consists of multiple-step intracellular process in degradation pathway that involves the delivery of cytoplasmic cargo to lysosomes (59). Autophagy showing double-membrane vesicles containing organelles and the other contents in cytoplasm was described as its characteristic under electron microscope observations (52). Whereas autophagy is a simple and nonspecific process in degradation pathway, recent data have demonstrated that it specifically sequesters damaged mitochondria to prevent the release of cytochrome C that activates the intrinsic apoptosis pathway (85). Autophagy is a basic mechanism to remove damaged organelles and long-lived proteins. Inefficiency of this process is linked to human pathophysiological conditions including neurodegenerative disease, muscle disease, cancer, immunity, and host pathogen interaction (59). Unlike apoptosis pathway extensively has been studied since the early 1990s, autophagy has emerged in past ten years even though it was first introduced approximately 40 years ago (47). Although this has been a rapid increase in the number of autophagy-related publications, our understanding of autophagy is limited and many challenging questions are waiting to be answered.

Autophagy is a dynamic and, multi-step process regulated at several steps (48). A cell maintains homeostasis at a low basal level of autophagy, but it is rapidly upregulated to generate more energy and nutrients during starvation, undergo architectural remodeling during differentiation, and remove damaged bulk of cytoplasm during

oxidative stress (92). Two major effectors play significant roles as nutrient sensors in autophagy modulation. The target of rapamycin (TOR) shuts off autophagy by integrating the signals from upstream pathway including insulin, growth factor, and mitogen (upstream and downstream of mTOR). The eukaryotic initiation factor 2α (eIF2α) kinase Gcn2 and its downstream target Gcn4, a transcriptional tranactivator, turn on autophagy-related genes (Atgs) during starvation (92). The whole process of autophagy starts with the formation of autophagosomes and ends up with lysosomal fusion (74). Approximately 17 Atg proteins, first described in yeast, are essential in induction, generation, maturation, and recycling of autophagosomes (49).

Autophagy and its cell survival mechanism

Recent evidence suggests that autophagy is required to maintain cell survival. Deltetion of Atg genes results in the loss of cell survival protection during nutrient depletion. When nutrient is depleted, cells employ autophagy to convert the source of metabolic substrates to maintain cellular activity (104). Recent studies have shown that organisms lacking Atg genes have increased cell death. In C elegan model, silencing of Beclin-1 and Atg-7 results in reduction of autophagy in the pharyngeal muscle and survival of wild-type worms after nutrient depletion (41). Several studies intended to elucidate the function of Atg proteins on survival modulation. Levin and coworkers indicated that autophagy genes are implicated in lifespan control (67). Silencing of Atg6 (BEC-1) with RNAi inhibits the lifespan extension in mutants by reducing DAF-2/IGF-1 receptor activity. Depletion of Atg-7 and Atg-2 suppresses the long-lived phenotype of *daf-2/Igf-1* mutant nematodes (34). These results indicated the important role of autophagy pathway on promoting longevity. Not only is autophagy able to maintain

cellular homeostasis during starvation, but also enhance removal of damaged mitochondria, other organelles, and protein aggregation. These fundamental mechanisms are also utilized in various cellular pathways that are critical in rescuing cells during aging, neurodegenerative process, and infection (48). Not only normal cells but cancer cells also take advantage of autophagy. Under limited blood supply, autophagy may provide the source of energy to promote tumor development. Recent findings demonstrate that over-activation of the Ras signaling pathway observed in several types of cancers enhances autophagy, allowing solid tumors to survive until vascular support can be established (17). However, the function of autophagy to enhance cell survival is a self-limited process. The starving cells will eventually commit to die of necrosis due to energy depletion.

Autophagy: another pathway for cell death

Mutilcellular organisms control their cell numbers by elimination of abnormal damaged cells. Two major types of programmed cell death have been differentiated by morphological criteria. Type I cell death or apoptosis is defined by the presence of nuclear condensation and fragmentation without major ultrastructural changes in organelles, while Type II cell death (autophagy) is characterized by accumulation of autophagosomes in the cytoplasm (4). It has been known that a cell can manifest large-scale autophagy shortly before or during their death, but the underlying mechanisms in autophagic cell death are still unclear. In addition, autophagy has been proposed as an alternative and efficient death pathway in apoptosis-resistant tumor (3). Apoptosis–defective cells (Bax^-/Bak^-) with double knockout of Bax and Bak genes have been widely used to determine the association between apoptosis and autophagy. Instead of

undergoing apoptosis after exposure to a variety of apoptotic stimuli, cytoplasm of Bax-/Bak- double knockout cells were filled with numerous double membrane vesicles, which have been confirmed to be autophagosomes by the punctate distribution of GFP-LC3 (108). These results indicated that autophagosome formation was required for certain cell death and that there is an alternative death mechanism other than apoptosis pathway. Tsujimoto and colleagues (115) demonstrated that Bax^-/Bak^- cells committed to death accompanied by autophagic vesicles when treated with etoposide (a cancer drug inhibiting topoisomerase II) or staurosporine (an antibiotic drug preventing ATP binding to the kinase). In addition, silencing of Atg 5 or Beclin 1 was able to relieve the presence of autophagosomes and cell death. Consistently, Lenardo and colleagues (115) reported that human U937 and mouse L929 cells that were treated with a pancaspase inhibitor (zVAD) underwent non-apoptotic cell death with the presence of autophagosomes, which is inhibited by RNAi- mediated knockdown of Atg5 and 7. The report showed that caspase and apoptosis inhibitor, zVAD, can inhibit autophagy pathway (111). Dual inhibition by zVAD leads cells to die via necrosis because apoptosis and autophagy are simultaneously inhibited. A recent study showed that induction of autophagy by nutrient depletion resulted in a significant protection against zVAD-induced cell death, and knockdown of Atg 5, 6, or 7 markedly sensitized L929 cells to zVAD-induced death. This suggests that autophagy helps a cell to survive and that inhibition of lysosomal function in autophagolysosomes promotes zVAD-induced necrotic cell death (113). These observations are potentially important in developing novel therapeutic strategies for several diseases that involve the modulation of autophagy (51). In cancer treatment, drugs inducing autophagy become more widely used in clinical practice. Treatment of

MCF7 breast carcinoma cells with tamoxifen, an estrogen receptor blocker, leads to autophagic cell death rather than apoptosis. Although the underlying mechanism is still not clear, it is speculated that tamoxifen-induced autophagy leads to cell death due to its failure to restore normal function to cells (9).

Cross talking between autophagy and apoptosis

Several lines of evidence have indicated that autophagy acts as a decision marker when apoptosis is crippled. In MCF-10A cells expressing anti-apoptotic proteins, apoptosis induction via TRAIL stimulated autophagic cell death (69). This result implies that regulations of autophagy and apoptosis must be coordinated. In addition, the proteins shared in the central component of apoptosis and autophagy machinery such as Bcl-2 family proteins and FADD also involve both processes (81). Beclin 1/Atg6, an autophagy protein playing a role during autophagosome formation, has been considered as a connector between autophagy and apoptosis. Bcl-2 family proteins are the major target of Beclin1 to inhibit apoptosis. The interaction between Bcl-2 and Beclin 1 results in failure of binding between Bcl-2 and Bax, resulting ininhibition of the release of cytochrome C that directly activates caspases and eventually leads to cell death via intrinsic apoptosis (27). Consistently, Kromer and his group also showed that the disruption of interaction between Beclin 1 and Bcl-2 protein family can enhance autophagy. It has been suggested that Bcl-2 as an anti-apoptotic protein also regulates autophagy as well (63). Although the underlying mechanism remains unclear, a study showed that Bcl-2 can block the release of calcium from the ER, which inhibits mTOR and activates autophagy (35). Not only does intrinsic apoptotic pathway involve in autophagy modulation, but extrinsic apoptosis pathway can serve as a key player as well.

Autophagy can be easily observed when apoptosis is blocked, indicating that autophagy and apoptosis are able to be induced through FADD (102). The study indicates that component of apoptosis machinery regulating both extrinsic and intrinsic pathways can also modulate autophagy.

The balance in dual roles of autophagy

Autophagy regulates two opposite fates; cell survival and death, by either its pro-survival or pro-death role. During nutrient depletion, autophagy suppresses apoptosis and promotes cell survival. On the other hand, Autophagy also functions as a type 2 programmed cell death when cell survival cannot be maintained. In the fly, steroid controls the transcription regulator BR-C, E74A, and E93 to trigger autophagic cell death in *D. melanogaster* salivary glands (57). Inhibition of caspases and external apoptotic stimuli can also induce autophagic cell death (69). Although it is not well understood how autophagy makes its decision between cytoprotective and cytotoxic outcome, it is strongly suggested that the balance in input from signaling pathways drive cells to either survive or die. Perhaps some underlying mechanisms are essential to switch on when autophagy undergoes beyond the point of no return and commits cells to death. The connection between the dual roles of autophagy on cell survival and death requires better understanding.

Autophagy and herpesviral infections

The best-characterized evidence of autophagy in host-pathogen interactions was described in engulfment of *Mycobacterium tuberculosis* in phagosomes and the trapping of cytosolic group A streptococci in autophagosomes. It implies that autophagy is a

protective mechanism against infection through destroying the pathogens in autolysomes that contain several enzymes such as acid hydrolase and lysozyme (18). Whereas facing a number of host defense mechanisms, pathogenic organisms employ various strategies to evade host defenses. In HSV-1, the ICP34.5, a neurovirulent protein interfering with PKR antiviral activity, can inhibit autophagy (18). This results in the preventing of the degradation of viral particles. Besides immune evasion, viruses also employ autophagy in different ways in order to gain advantages from host cells. Several studies indicate viruses replicate by evading or subverting the autophagy pathway. Interestingly, KSHV employs replication and transcription activator (RTA), an important viral protein for lytic reactivation, to enhance autophagosome formation and autophagosome fusion. The underlying mechanisms and reasons for enhancing autophagy remain unclear. However, it has been shown that RTA can induce protein degradation by ubiquitination pathway, which might be consistent with the function of autophagy on protein turnover process (109). Another KSHV protein that has been well studied is KSHV vFLIP, a protein expressed during latent infection. A number of previous studies have shown that this protein plays arole in inhibiting apoptosis and promoting cell transformation. KSHV vFLIP is involved in suppression of autophagosome formation by interacting with LC3 protein to inhibit autophagic cell death (58).

Chapter 3: Materials and Methods

3.1 *Cells and virus*

3.2 *Apoptosis and autophagy induction*

3.3 *Antibodies*

3.4 *Plasmids and vectors*

3.5 *Transfection*

3.6 *Fluorescence microscope*

3.7 *Western blot analysis*

3.8 *Cell viability assay*

3.9 *Activity assay of Caspase-8,-9,-3, and -7*

3.10 *NF-κB reporter assay*

3.11 *Subcellular fractionation*

3.12 *Establishment of siRNA*

3.13 *Real-time PCR*

3.1 Cells and viruses

Cell lines HeLa and HEK293 were maintained in Dulbecco's modified Eagle's medium *(*DMEM) supplemented with 10% fetal bovine serum (FBS). Transfection of the cells was done with GeneExpresso 8000 (Lab Supply Mall, Gaithersburg, MD) as per the manufacturer's instructions. Cell line RhF was a gift from B. Damania (21) and maintained in DMEM supplemented with 10% FBS. RRV 26-95 was a gift from R.C. Desrosiers (7) and propagated in RhF cells. BJAB was maintained in RPMI1640 medium supplemented with 10% FBS. Stable HeLa cells expressing CFP-LC3 has been described previously (83) and maintained with DMEM supplemented with 10% FBS and G418 (Invitrogen, Carlsbad, CA) at 400 µg/ml.

Establishment of RRV vFLIP-expressing stable HeLa cell line

We generated HeLa cells stably expressing RRV vFLIP fusing with yellow fluorescence protein (YFP). Briefly, HeLa cells were transfected with VenusN1-vFLIP and the cells containing the plasmid were selected in medium supplemented with G418 (Invitrogen) at 400 μg/ml. Fluorescence-activated cell sorting was conducted to enrich cells with YFP expression. Sorted cells were plated and cultured to expand cell population. The sorting and expanding process was repeated three times to enrich and stabilize the cells with YFP expression. The vFLIP expression was confirmed with Western blotting analysis using rabbit anti-vFLIP antibody. The stable HeLa cells were stored in a liquid nitrogen container and used in this study.

3.2 Apoptosis and autophagy induction

Apoptosis induction

Tumor necrosis factor-α (TNF-α) (R&D Systems, Minneapolis, MN) and cycloheximide (Sigma) were added to cells at final concentrations of 50 ng/ml and 2.5 μg/ml, respectively, to induce apoptosis. The cells were harvested at different time points after apoptosis induction for RNA isolation or Western blotting analysis, as indicated. Either TNF-α or cycloheximide alone at their respective concentrations used in this study cannot induce apoptosis. To inhibit the autophagosome formation step in autophagy, cells were treated with 3-MA (Fisher) at a final concentration of 10 mM for one hour before apoptosis induction. To interrupt degradation of autophagosomes in lysosomes, cells were treated with ammonium chloride (Fisher) at a final concentration of 20 mM at 4, 6,

and 8 h after apoptosis induction. At 10 h after apoptosis induction, the cells were harvested for Western blotanalysis.

Autophagy induction

Rapamycin (R&D Systems) was added to confluent monolayer HeLa-LC3 stable cells at 4 μM final concentration to induce autophagy. The cells were fixed with 1% paraformaldehyde for confocal fluorescence microscopy at 6 and 9 h after the drug treatment or harvested for Western blot analysis, as indicated.

3.3 Antibodies

Preparation and purification of antibody against RRV vFLIP

RRV vFLIP was expressed in BL21 *E. coli* cells as a fusion protein of vFLIP-GST from pGEX-3X-vFLIP plasmid with the induction of 1 mM IPTG (Promega, Madison, WI). The vFLIP-GST fusion protein was purified by B-PER GST Fusion Protein Purification Kits (Fisher Scientific, Pittsburgh, PA) according to the manufacturer's instructions. Purified vFLIP-GST fusion protein was used to immunize rabbits for vFLIP antibody preparation (GenScript Corporation, Piscataway, NJ). Rabbit anti-vFLIP antibody was purified from the antiserum by affinity-purification with CarboxyLink^{TM} Kit (Fischer Scientific), which was used to covalently link purified vFLIP-GST fusion protein to agarose beads. The vFLIP antibody was verified by detection of vFLIP expressed in HeLa cells in Western blotting analysis.

Commercial antibodies

The antibodies used to detect the level of cellular proteins in this study are against PARP-1, caspase-8, caspase-9, and NF-κB p65 (Santacruz biotechnology, Santa Cruz, CA); LC3 (Cell signaling); β-tubulin, GFP, and GST (Sigma)

3.4 Plasmids and vectors

The plasmid Venus-N1 and VenusC1 vectors that contain an improved version of yellow fluorescent protein named "Venus". The N1 and C1 nomenclature of the Venus vector indicates the location of the mutli-cloning sites upstream and downstream of the Venus gene, respectively. The PGEX-3X vector (GE Healthcare) was used for expression of RRV vFLIP-GST fusion protein in BL21. The plasmid pGL4.32 [NF-ΚB-RE/Hygro], purchased from Progmega®, was used in NF-κB reporter assay.

Construction of vetctor expressing RRV vFLIP

Supernatant of RRV-infected RhF cells containing RRV DNA was used as template to amplify RRV ORF71 gene. PCR products were generated with primers R71F2 and R71R3 (Table 1), which contain restriction sites of *Eco*RI and *Bam*HI, respectively, for directional cloning into VenusN1 vector, as previously described (42). In addition, PCR products amplified from primers R71F2 and R71R2 (Table 1) were cloned into VenusC1 vector. All clones were confirmed by restriction enzyme digestion and DNA sequencing. ORF71 was cloned upstream and downstream of Venus in VenusN1 and VenusC1, respectively. The expression of fusion proteins of vFLIP and Venus were easily observed under fluorescence microscope. As for protein expression in prokaryotic system, ORF71 gene was amplified with primer R71F1 and R71R1 (Table 1) that contain restriction site

of *Bam*HI and *Eco*RI, respectively, and cloned into pGEX-3X vector. Furthermore, ORF71 gene was also cloned into pCMVTag2C and pCDNA3 vector. All clones were confirmed by DNA sequencing. To study the function of truncated proteins of RRV vFLIP, fragments of ORF71 was cloned into VenusN1 vector to generate four plasmids with different primers (Table 1). All clones were verified for the presence of inserts by DNA sequencing. Construction of CFP-LC3 plasmid has been recently reported (65). Construction of mCherry-LC3 plasmid has been previously described (83).

Table 1. Oligonucleotide used in generation of plasmids for expression of RRV vFLIP, truncated vFLIP proteins, and siRNA against vFLIP mRNA

a. F, forward; R, reverse.
b. Restriction sites of *Bam*HI, *Xho*I and *Eco*RI included in the primers are italicized

Primer[a]	Sequence (5' to 3')[b]	Plasmid
R71F1	GC*GGATCC*TGTTCCCGCATAAGCGGTT	pGEX-3X
R71R1	GA*GAATTC*TTAACCGGGTGCGTTGGCG	
R71F2	GC*GAATTCC*ATGTTCCCGCATAAGCGGTT	VenusC1-R71
R71R2	GA*GGATCC*TTAACCGGGTGCGTTGGCGG	
R71F2	GC*GAATTCC*ATGTTCCCGCATAAGCGGTT	VenusN1-R71
R71R3	GA*GGATCCG*AACCGGGTGCGTTGGCGGC	
R71F8	GGG*CTCGAG*ATGTTCCCGCATAAGCG	VenusN1-R71D1
R71R7	CC*GAATTC*GAATGGAGAGCATCAGGTG	
R71F8	GGG*CTCGAG*ATGTTCCCGCATAAGCG	VenusN1-R71D2
R71R8	GC*GAATTC*GCAGGTCACTTAAAACCATG	
R71F10	GCG*CTCGAG*ATGTACAAACACCTGATGC	VenusN1-R71D3
R71R9	GC*GAATTC*GACCGGGTGCGTTGGCGGC	

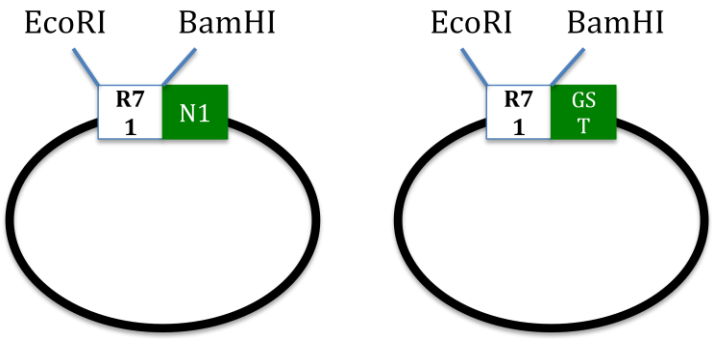

Figure 2. Construction of RRV ORF71 expression plasmids. The ORF71 of RRV was cloned into VenusN1 vector, upstream of the Venus reporter gene (N1-R71) using the indicated restriction enzymes. In addition, ORF71 was also cloned into pGEX-3X vector to generate purified protein for antibody production.

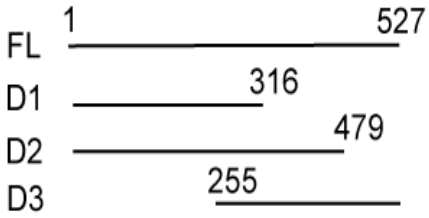

Figure 3. Schematic Illustration of the truncations of ORF71. Three vFLIP fragments were designed and cloned into VenusN1 vector, designated as D1, D2, and D3, respectively. Numbers above lines indicate nucleic acid bases of vFLIP open reading frame. FL: full length.

3.5 Transfection

Transient transfection was conducted on HEK293 and HeLa cells grown to 90-95% and 65-70% confluence, respectively in 12-well plates. As for 293 cells, 8 μl polyethylenimine (polysciences) was mixed with 2 μg of plasmid or empty vector DNA

in a volume of 100 μl of DMEM-RS (Hyclone) per well. For transfection of HeLa and RhF cells, 2 μg plasmid DNA was mixed with LF2000 (Invitrgoen), according to the manufacturer's instructions. Cells treated with only the transfection reagent were served as mock-transfection controls. Cells were harvested at 18 to 24 h after transfection for protein expression unless indicated in text at different time points.

3.6 Confocal fluorescence microscopy

Cells were seeded directly onto cell culture plates containing coverglass, incubated overnight, and transfected the next day. At 24 h post transfection, the coverglass was observed directly under confocal fluorescence microscopy or fixed with 1% paraformaldehyde and mounted onto slide with anti-fade mounting solution (Invitrogen) before observation.

3.7 Western blot analysis

Cells were transfected with either VenusN1-vFLIP or VenusN1 vector. At 24 h post-trasnfection, the cells were harvested with Laemmli sample buffer. The whole proteins in cell lysates were separated onto 12% polyacrylamide gel. The proteins were transferred to nitrocellulose membrane and probed with rabbit anti-vFLIP antibody. Specific signal through the reaction of horseradish peroxidase isoenzyme with hydrogenperoxide and chemiluminescence substrate were detected by using ChemiDoc XRS imaging system (Bio-Rad Laboratories, Hercules, CA). Beta-tubulin was detected on the same blot membrane to normalize protein loading. Digital image acquisition and densitometry analyses were conducted using Quantity One program (Version 4.6) (Bio-Rad). Likewise in other experiments, the expression of other proteins was detected with antibodies as

follows; GST (Rockland Immunchemicals Inc., Gilbertsville, PA), GFP, β-tubulin (Sigma), LC3 (Cell Signaling Technology, Danvers, MA), NF-κB p65, PARP-1, and caspase-9 (Santa Cruz Biotechnology, Santa Cruz, CA).

3.8 Cell viability assay

Cells viability was determined with CellTiter-Glo Luminescent Cell Viability Assay (Promega). The ATP level in cells associates with the number of viable cells in culture. This method was conducted to measure the amount of ATP in cells before and after apoptosis induction and nutrient starvation. As for apoptosis experiment, cells cultured in 96-well plate were induced to undergo apoptosis for 4 h prior to addition of Cell titer-Glo reagent and incubated for 10 minutes at room temperature. For nutrient starvation, the cells were seeded into a 12-well culture plate and incubated overnight at 37°C. On next day, the culture medium was then replaced with Hank's Balanced Salt Solution (HBSS). The cells were observed under a microscope before harvesting at 0, 24, and 48 h after the addition of HBSS. The luminescence signal generated from luciferase reaction was measured with a VICTOR^3 Multilabel Counter (Perkin-Elmer, Waltham, MA). Relative percentages of luminescence intensity were analyzed by comparison to mock-treated controls.

3.9 Caspase activity assay

Activities of caspase-3, -7, -8, and -9 were measured by using Caspase-Glo 3/7, Caspase-Glo 8, and Capase-Glo 9 Assay kits (Promega). Cells seeded onto a 96-well culture plate were induced to undergo apoptosis for 4 h prior to testing of caspase activities. Caspase-Glo reagent was added to the cells and incubated for 30 minutes at

room temperature. The luminescence signal was measured and converted to the relative percentages of luminescence intensity, which was compared with controls.

3.10 NF-κB reporter assay

HeLa cells were co-transfected with pGL43.2 [*luc2p/ NF-κB/*Hygro] Vector (Promega) that contains a NF-κB responsive element driving transcription of luciferase reporter gene and either VenusN1-vFLIP or VenusN1 empty vector. VenusC1-vFLIP and VenusC1 plasmids were also included in this assay. Plasmid pRL-TK (Promega) was used as an internal control for all transfection. As for positive control, cells were induced with TNF-α (at concentration of 50 ng/ml) in order to activate the transcolation of NF-κB. For negative control, a prokaryotic vector pGEX-3X was used to co-transfect with NF-κB reporter vector. Dual-Glo Luciferase Assay System (Promega) was used to detect luciferase activity at 4 h after TNF-α addition following the manufactuer's instructions. The change in the activity of lucicerasewas determined by comparing the normalized luciferase activity in treated versus untreated transfectants in terms of relative folds.

3.11 Subcellular fractionation

Nuclear fraction was extracted from normal HeLa and HeLa-VFLIP stable cells using the CelLytic NuCLEAR Extractino Kit (Sigma). Cell were collected, lysed, and fractionated by following manufacturer's instructions. The nuclear and cytoplasmic fractions were subjected to Western blot analysis. Antibodies against cytoplasmic protein (β-tubulin) and nuclear protein (PARP-1) were utilized to assess the success of subcellular fractionation.

3.12 Design and testing of siRNA

siRNA Target Designer (version 1.6) was used to design siRNA against ORF71 mRNA, according to manufactuer's instruction (Promega). Short duplex DNA oligonucleotides containing T7 polymerase promoter upstream of either the sense or antisense DNA sequences of siRNA against ORF71 of RRV were used as a template to generate siRNA using T7 RiboMAX^{TM} Express RNAi system (Promega). Briefly, oligonucleotides were annealed to generate either sense or antisense RNA template. Two separated RNA templates were assembled for each siRNA after transcription. The silencing effect of siRNA against ORF71 was tested by co-transfection with Venus-N1-vFLIP in 293T cells. Cells with Venus expression were observed under fluorescence microscope. The mRNA level of ORF71 was also determined in RRV-infected BJAB cells by Real-time PCR.

3.13 Real-time PCR

Total RNA was isolated from cell lysed with TRIzol® Reagent (Invitrogen). RNA was treated with RNase free –DNAse (Promega) to remove carryover DNA from RNA isolation procedure. RNA transcription was conducted using AMV reverse transcriptase and random hexamer (Promega). Real-time PCR primers designed based on cDNA sequences of target mRNA are shown in Table 2. Real-time PCR with SYBR Green detection was done as described previously (78). The gene expression level in vFLIP-expressing cells was quantified by $2^{-\Delta\Delta CT}$ method in comparison with a control of cells with empty vector.

Table 2. Oligonucleotides used in real-time PCR

a. F, forward; R, reverse

Primer[a]	Sequence (5’ to 3’)
MnSOD-F1	GGAGAAGTACCAGGAGGCGT
MnSOD-R1	TAGGGCTGAGGTTTGTCCAG
Actin-F1	ATCGTGCGTGACATTAAG
Actin-R1	ATTGCCAATGGTGATGAC

CHAPTER 4: RESULTS

4.1 Cloning and expression of RRV ORF71 gene

RRV ORF71 was cloned into pGEX3X vector for expression of vFLIP-GST fusion protein. The expression of the protein was detected with mouse anti-GST antibody. The fusion protein was purified and used to immunize rabbits for antibody preparation. The rabbit antibody against vFLIP was purified by affinity chromatography and confirmed for its specificity in Western blot analysis with vFLIP-GST protein.

The expression of vFLIP fusion protein occurs both in the cytoplasm and nucleus in a diffuse or homogenous pattern, when observed under confocal microscopy. In RhF cells transfected with VenusN1-vFLIP, vFLIP fusion protein mainly localizes in the nucleus, while a similar cellular distribution pattern was clearly observed in HeLa cells (Fig 4). The result observed in RhF cells was consistent with the previous studies of vFLIP of KSHV. HEK293 cells were transfected with VenusN1-vFLIP or empty vector. The vFLIP-Venus fusion protein was detected by a mouse monoclonal antibody against GFP and the size of the fusion protein was approximately 45 kDa, while cells transfected with the empty vector yielded a band at 25 kDa as expected (Fig 5A). Western blot analysis of the cell lysates with the rabbit anti-vFLIP antibody detected the 45 kDa fusion protein, while no signal was visible in whole proteins from cells transfected with empty vector demonstrating the specificity of the antibody against vFLIP (Fig 5B). These results confirmed the expression of vFLIP fusion protein in transiently transfected cells. Our attempt to express vFLIP in other vectors with FLAG tag or without Tag, such as pCMV-Tag and pCDNA3, was unsuccessful. Expression of vFLIP from such plasmids was

below detection level in transiently transfected cells by IFA or Western blot. However, the expression of RRV vFLIP from pcDNA3-vFLIP was clearly detected when a cell-free transcription and translation system was used. This indicates that the vFLIP protein was very unstable or short-lived and the fusion with Venus enhances the stability of vFLIP.

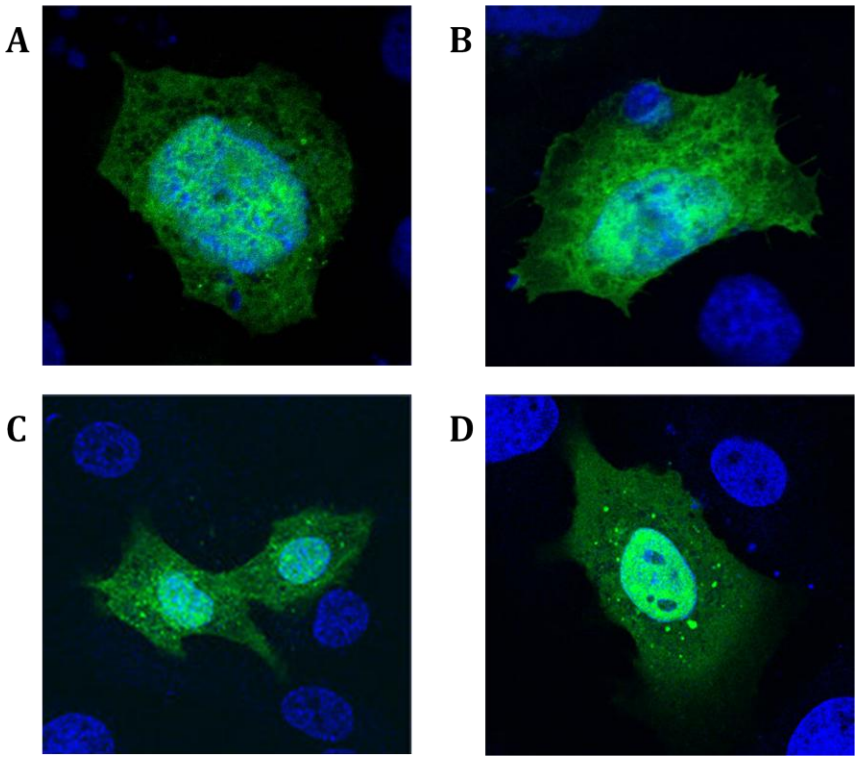

Figure 4. Subcellular localization of RRV vFLIP fusion with YFP. The cells were transfected with VenusN1-vFLIP or empty vector (EV). A. HeLa cell transfected with empty vector. B. HeLa cell transfected with VenusN1-vFLIP. C. RhF cells tranfected with empty vector. D. RhF cells tranfected with VenusN1-vFLIP.

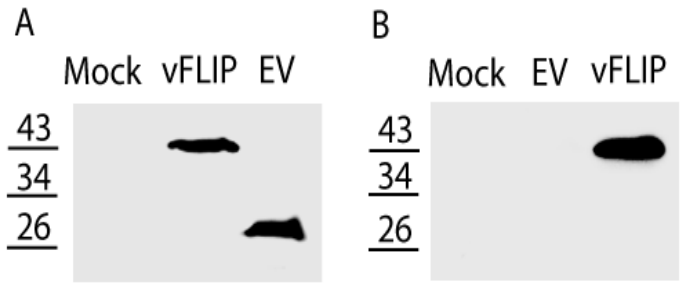

Figure 5. Detection of RRV vFLIP protein by Western blotting analysis. The cells were transfected with VenusN1-vFLIP or empty vector (EV). A. Detection of vFLIP-Venus fusion protein by mouse anti-GFP antibody. B. Detection of vFLIP-Venus fusion protein by rabbit anti-vFLIP antibody. Molecular weight markers are indicated on left of the images.

4.2 RRV vFLIP inhibits apoptosis

Since two death effector domains have been shown anti-apoptotic function in sereral vFLIPs, we tested RRV vFLIP effect on apoptosis pathway. HeLa and HeLa-vFLIP stable cells were induced to undergo apoptosis with TNF-α and cycloheximide, and harvested at 0, 6, 9, and 12 h after the treatment. Cleavage of PARP-1 was assessed. PARP-1 is a nuclear DNA-binding zinc finger protein that influences DNA repair and apoptosis. PARP-1 proteolytic cleavage is considered as a classical hallmark for apoptosis. The strong PARP-1 cleavage bands at 89 kDa were clearly observed in control HeLa cells at 6, 9 and 12 h after apoptosis induction, while not detectable in the cells expressing vFLIP The apoptosis induction leads to the cleavage of inactive pro-caspases to active caspases. We detected pro-caspase 9 level in the cells and noticed that the level of pro-caspase 9 was serially decreased after 6 to 12 h in HeLa cells. However, vFLIP

expression did not lead to much change in precursor caspase 9 (Fig 6). The results indicate that vFLIP inhibits apoptosis.

To further confirm the vFLIP effect on apoptosis signaling, we conducted caspase activity assays at 6 h after the apoptosis induction. Caspase activities of caspase 3/7, 8, and 9 in vFLIP-positive cells were 55%, 13% and 58% lower, respectively, than those in control HeLa cells(Fig 7). The caspase 9 and caspase 3/7, representing an initiation factor of intrinsic apoptosis pathway and executive factors, respectively, were effectively inhibited, although we did not observe much change of caspase-8 activity. The reduction of caspase activities of caspase-3, -7 and -9 in HeLa-vFLIP cells may account for the minimal cleavage of PARP-1.

Reactive oxygen intermediates play a critical role in apoptosis induced by TNF-α and cycloheximide and overexpression of manganese superoxide dismutase (MnSOD) prevents apoptosis (32) . Superoxide dismutases (SOD) are a class of enzymes that catalyze the dismutation of superoxide into oxygen and hydrogen peroxide. Three forms of superoxide dismutase are present: SOD1 is located in the cytoplasm, SOD2 in the mitochondria, and SOD3 is extracellular. SOD2 has manganese in its reactive centre and is also known as MnSOD (66). The transcripts of several genes in apoptosis pathway including Bax, Bad, Bid, and MnSOD were assessed by real time RT-PCR at 4 h after apoptosis induction. Only MnSOD expression was highly up-regulated to almost 90 folds in HeLa-vFLIP stable cells as compared with control (Fig 8). The MnSOD elevation was consistent with the reduction of caspase-9 activity and unchanged procaspase-9 level in vFLIP-stable cells. Reactive oxygen species are directly involved in intrinsic apoptosis by increasing the threshold of mitochondria outer membrane permeability. This results in the

leakage of cytochrome C from mitochrondria which further activates the cleavage of active caspase-9.

Our data above shows that RRV vFLIP inhibits signaling cascade of apoptosis pathway. To test whether the anti-apoptotic function of vFLIP is sufficient to protect the cells from apoptotic cell death, the HeLa-vFLIP stable cells were treated with TNF-α and cycloheximide to induce apoptosis. Cell viability assay was conducted at 0 and 38 h after the apoptosis induction. Compared with normal HeLa cells at 0 h, relative cell viability of HeLa-vFLIP stable cells at 38 h after apoptosis induction was 0.85-fold, while that of the control cells was 0.43-fold, similar to 0.39-fold of un-transfected HeLa cells. This result indicates that vFLIP expression can protect the cells against apoptosis (Fig 9).

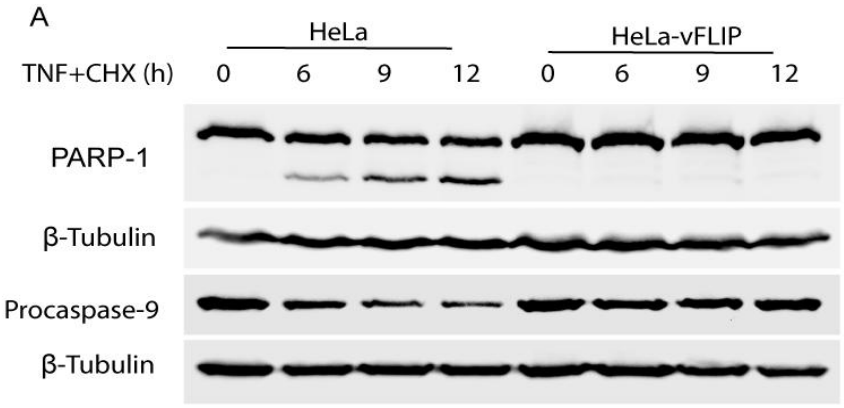

Figure 6. Detection of PARP-1 and Procaspase-9 by Western blot analysis. HeLa and HeLa-vFLIP stable cells were treated with tumor necrosis factor-α (TNF-α) and cycloheximide to induce apoptosis, and harvested at 0, 6, 9, and 12 h after the treatment. PARP-1 cleavage was detected as a marker of apoptosis. Cleavage of procaspase-9 indicates activation of caspase 9, an initiator of apoptosis. Tubulin was detected on the same membrane for loading normalization.

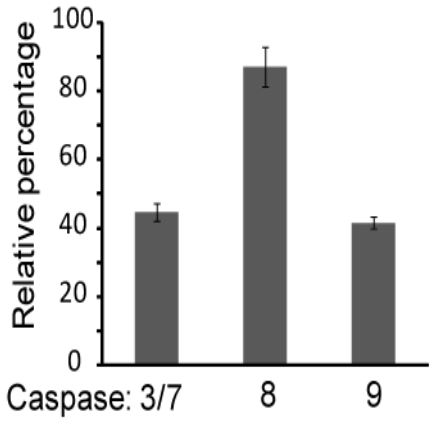

Figure 7. Activity assay Caspase-3,-7,-8, and -9. HeLa-vFLIP stable cells and HeLa cells were treated with TNF-α and cycloheximide for 6 h. Relative percentages of caspase activities in comparison with normal HeLa cells are shown. Significant differences between HeLa-vFLIP and HeLa cells are denoted by "**", which indicates $P < 0.01$.

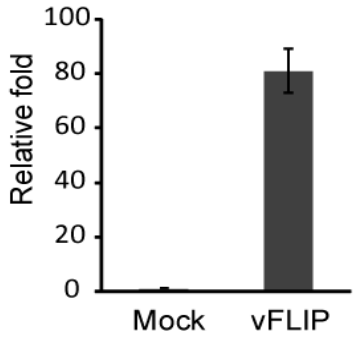

Figure 8. Detection of MnSOD transcript in HeLa-vFLIP stable cells after apoptotic induction. Real time PCR was conducted. Relative fold in comparison with normal HeLa cells under the same treatment is shown.

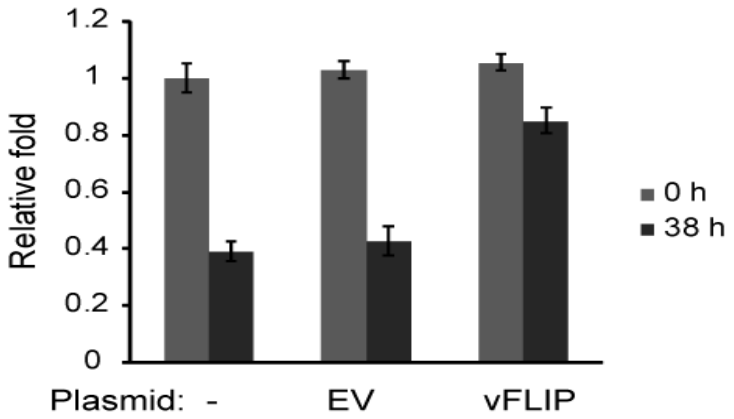

Figure 9. Cell viability assay of HeLa cells. HeLa-empty vector (EV) and HeLa-vFLIP cells at 0 and 38 h after apoptosis induction. Relative folds in comparison with normal HeLa cells at 0 h are shown. Significant differences between HeLa-vFLIP and HeLa-EV cells are denoted by "**", which indicates $P < 0.01$.

4.3 RRV vFLIP does not activate NF-κB pathway

It is known that KSHV vFLIP strongly activates NF-κB signaling (11). Binding of KSHV vFLIP to IKK gamma induces phosphorylation and subsequent recognition by ubiquitinating enzyme system, which liberates NF-κB from association with inhibitory IKB proteins to nucleus. The nuclear translocation of NF-κB promotes transcription of a large number of genes involved in immune responses, inflammation, cell survival and cancer. To test whether RRV vFLIP has a similar role, we transfected HeLa cells with NF-κB reporter plasmid pGL4.32[LUC2P/NF-κB-RE/HYGRO] and VenusN1-vFLIP. VenusC1-vFLIP and empty vector were included in the test. TNF-α was included to activate NF-κB signaling as a positive control. The luciferase reporter assay showed that luminescence signals in cells with vFLIP expression was low and similar to cells transfected with empty vector, while TNF-α treatment of normal HeLa cells induced 12-

fold increase. TNF-α treatment of HeLa cells transfected with VenusN1-vFLIP induced 9-fold elevation (Fig 10). Transfection of HeLa cells with prokaryotic vector pGEX-3X did not affect the NF-κB activation after TNF-α induction. This result indicates that vFLIP is unable to activate NF-κB signaling.

To verify the finding in NF-κB luciferase reporter assay, we conducted subcellular fractionation of HeLa cells to determine NF-κB subcellular location. After NF-κB is activated by TNF-α, it translocates into the nucleus and activates the expression of myriad genes. HeLa and HeLa-vFLIP stable cells were untreated or treated with TNF-α. Addition of TNF-α and cycloheximide to one well was included as a control. The cells were harvested at 4 h after induction and fractions of nucleus and cytoplasm were separated. Western blot analysis with antibody against NF-κB p65 subunit showed that p65 remained in the cytoplasm ofthe cells with stable vFLIP expression, while addition of TNF-α or combination of TNF-α and cycloheximide led to p65 nuclear translocation (Fig. 11). This result suggests that vFLIP is unable to cause nuclear translocation of NF-κB. Detection of β-tubulin in cytoplasmic fraction only and PARP-1 in nuclear fraction only demonstrated the successful separation of cytoplasmic and nuclear fractions. The unique feature of KSHV vFLIP in NF-κB activation has subsequent implications to pathogenesis of Kaposi's sarcoma as well as malignant tumor caused by KSHV infection. The abolishment of NF-κB activation can reverse the protective effect of KSHV vFLIP against growth factor withdrawal-induced apoptosis. Although the underlying mechanism of NF- κB translocation mediated by KSHV vFLIP remains unclear, it was suggested that Bcl-X_L is involved in this process. Upregulation of this protein due to NF-κB has been shown to inhibit the processing of caspase-9, -6, and -8. However, besides Bcl-X_L, several

genes involved inapoptosis pathway are also upregulated including A1 cIAP, cIAP2, XIAP, and IEX-1. Strong evidence demonstrated that NF-κB activation mediated by KSHV vFLIP correlates with transforming ability. Rat-1 cells expressing KSHV vFLIP form colonies in soft agar, and nude mice injected with those cells developed tumor. These results suggest that NF-κB activation caused by KSHV vFLIP play an important role in the pathogenesis of KSHV associated malignancies by inhibiting apoptosis and promoting cell transformation.

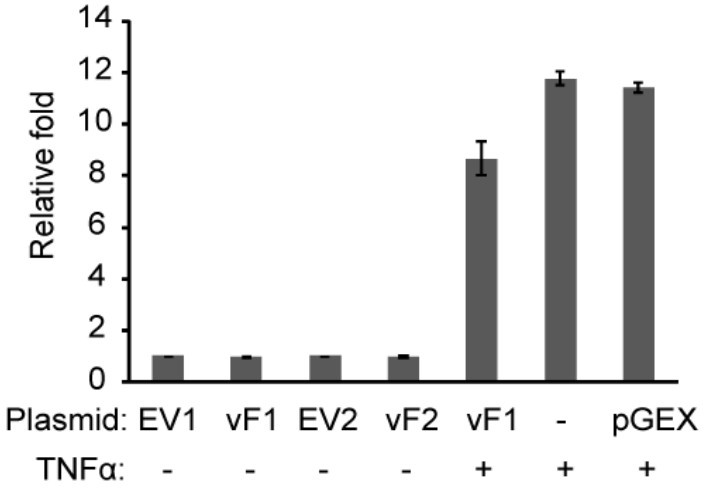

Figure 10. NF-κB reporter assay. HeLa cells were transfected with NF-κB reporter plasmid pGL4.32[LUC2P/NF-κB-RE/HYGRO], VenusN1-vFLIP (vF1), VenusC1-vFLIP (vF2), empty vector VenusN1 (EV1), or VenusC1 (EV2). TNF-α was used to activate NF-κB as a positive control. Prokaryotic expression vector pGEX-3X was included as a control. Luciferase signals were measured at 4 h after TNF-α addition. Relative folds in comparison with EV1 control are shown. There was no significant difference between vF1 and EV1 or between vF2 and EV2. Significant differences between cells with vF1 in

the presence or absence of TNF-α induction are denoted by "**", which indicates $P < 0.01$.

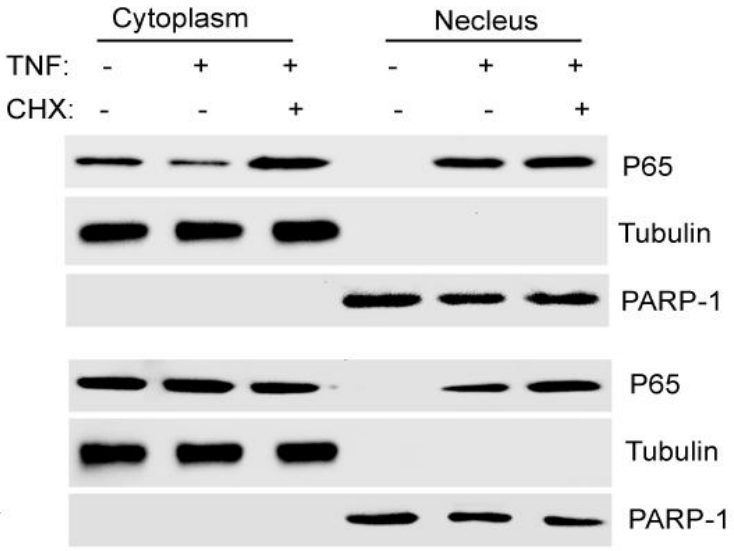

Figure 11. Subcellular fractionation to determine NF-κB nuclear translocation. HeLa cells (top panel image) and HeLa-vFLIP stable cells (lower panel image) were treated with TNF-α or combination of TNF-α and cycloheximide for 4 h and harvested for fractionation of cytoplasmic and nuclear portions, followed by Western blot analysis with p65 antibody. Tubulin and PARP-1 were detected on the same membrane to confirm the separation of cytoplasmic and nuclear fractions

4.4 Enhanced cell survival under starved condition in cells expressing vFLIP

Enhanced cell survival is one of the features of tumor cells. An increase of reactive oxygen species, depletion of nutrient, and waste product from rapid cell growth leads to hypoxic environment and nutritional stress to the cells, which interferes with cell survival. To determine whether RRV vFLIP can enhance cell survival under starved condition, we replaced cell culture medium of HeLa, HeLa-vFLIP, and HeLa-VenusN1

cells with HBSS. These cells were observed at 0, 24, and 48 h after HBSS addition and images were taken under bright field microscopy. HeLa-vFLIP stable cells survived longer than the other cells under starved condition, particularly at 48 h, the number of live vFLIP-stable cells were much more (Fig. 12A). Cell viability of vFLIP-stable cells was 1.24- and 1.58-fold higher than control HeLa cells at 24, and 48 h, respectively, after HBSS addition (Fig. 12B). The cells with empty vector had a slightly lower viability levels than control HeLa cells. This result indicated that RRV vFLIP might be involved in autophagy to extend cell survival as autophagy is a cell survival mechanism to turn over damaged organelles and long-lived proteins in the cytoplasm during starvation. It has been known that autophagy increases during starvation. This process allows cells to degrade long-lived protein and organelles so that they can obtain a source of macromolecular precursors such as amino acids, fatty acids, and nucleotides. Autophagy serves as a cell survival strategy to protect cells during nutrient deprivation. Strong evidence for the importance of autophagy in tumor cells was shown by an increase of autophagosome formation in the cells when deprived of growth/suvival factor. Knockdown of essential autophagic machinery component such as *Beclin 1/Atg6* gene sensitized cells to starvation-induced death. Furthermore, when autophagy was inhibited, those cells underwent apoptosis. This implies that autophagy that occurs under starved condition in tumor cells would prevent them from dying. Therefore, we would expect that vFLIP might employ autophagy pathway to promote the growth of cells and prevent apoptosis.

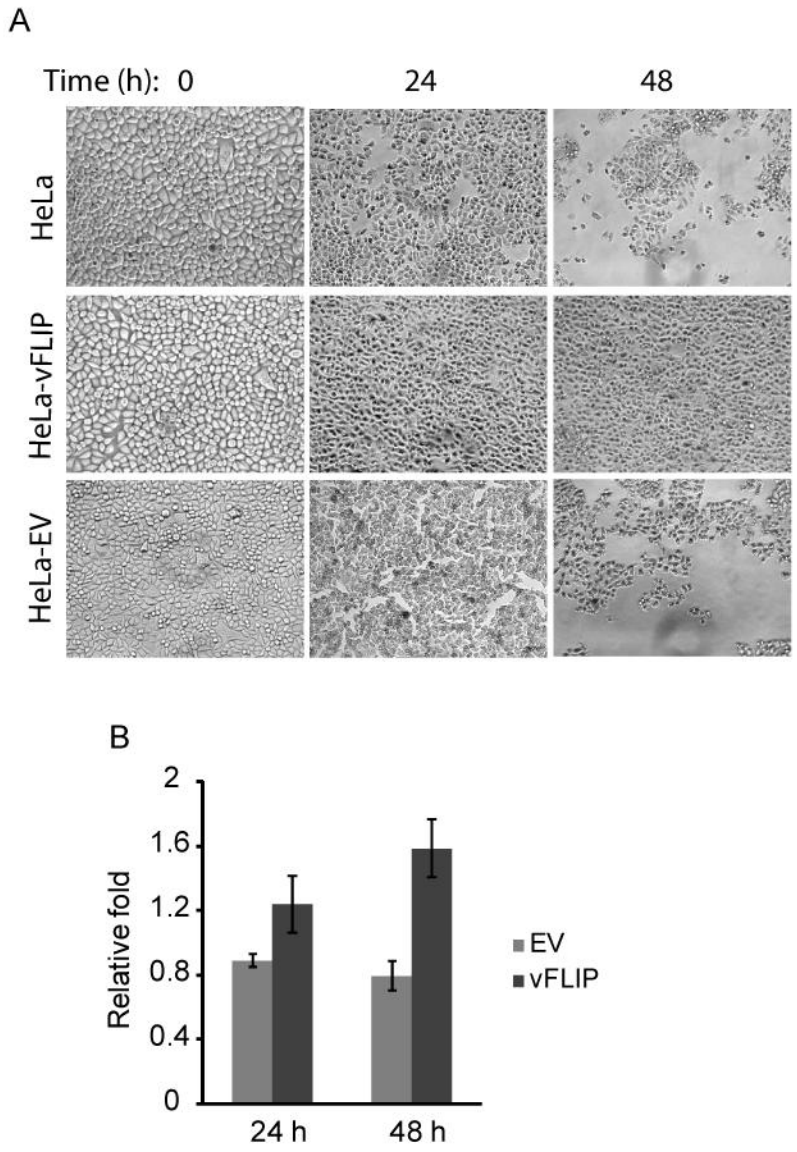

Figure 12. Effect of RRV vFLIP expression on HeLa cells under starved condition. A. Bright-field micrographs showing the cells under starvation at 0, 24 and 48 h. Normal HeLa, HeLa-vFLIP stable cells and HeLa-empty vector (EV) cells were starved after culture medium was replaced with Hank's balanced salt solution (HBSS). B. Cell viability assay of HeLa cells after starvation. The cells were assayed at 24 and 48 h after starvation by CellTiter-Glo Cell Viability Assay. Relative folds are shown in comparison with normal HeLa cells at 24, and 48 h, respectively, after normalization of cells at 0 h.

Significant differences between HeLa-vFLIP and HeLa-EV cells are denoted by "*" and "**", which indicate $P < 0.05$ and $P < 0.01$, respectively.

4.5 Elevation of autophagosome formation in cells with RRV vFLIP expressing after apoptosis induction

Autophagy is a dynamic and multi-step process and LC3-II has been widely used as a marker (65) . HeLa cells were co-transfected with VenusN1-vFLIP plasmid and mCherry-LC3 and, on next day, induced to undergo apoptosis with TNF-α and cycloheximide. The cells were observed for autophagosome formation after the apoptosis induction. The HeLa cells with vFLIP expression had more autophagosome punctates after apoptosis induction (Fig 13). The autophagosome punctates were more visible at 3 h after the apoptosis induction. The HeLa cells with vFLIP expression had more autophagosome punctates than control cells at both before and after apoptosis induction. For Western blot detection of LC3-II in the cells, HeLa and HeLa-vFLIP stable cells were transfected with CFP-LC3 plasmid and induced to undergo apoptosis the following day. The cells were harvested for western blot analyses at 0, 4, and 6 h after the apoptosis induction. The intensity of LC3-II band was used to assess autophagosome formation. A stronger LC3-II band was observed in HeLa-vFLIP stable cells than HeLa cells at all time points tested (Fig 14). Autophagic vacuolization before apoptotic death has been demonstrated in several mammalian cells including HeLa, Bax-/Bak- DKO, and MEF cells(1). The kinetic studies indicated that autophagic vacuolization preceded mitochondrion-dependent caspase activation in apoptosis. It has been shown that inhibition of caspases had no influence on autophagic vacuolization and mitochondrial changes. Therefore, RRV vFLIP's ability to reduce caspase activity might not be

responsible for an increase of autophagosome formation. The phenomenon of autophagosome formation drifts to a process marked by the conventional steps of apoptosis, which raise the question regarding the transitional phase between autophagy and apoptosis. In addition, autophagosome formation preceding apoptosis has been reported in *Drosophila* model system as well.

To determine whether autophagy plays a role in vFLIP's inhibition of apoptosis, we performed two experiments to inhibit autophagy at two critical steps; autophagosome formation and degradation of autophagosomes in lysosomes. HeLa-vFLIP stable cells were treated with 3-methyladenine (3-MA) for one hour before apoptotic induction to inhibit autophagosome formation. The cells were harvested at 10 h after apoptotic induction for Western blot analyses. The cleavage band of PARP-1 at 89 kDa was obviously observed in the cells treated with 3-MA, but not in mock-treated control (Fig 15). This result indicates that after 3-MA treatment of the cells, vFLIP could no longer protect the cells from apoptosis, and suggests that autophagosome formation is needed for the anti-apoptotic function of RRV vFLIP, which is consistent with the observation of a significant increase of autophagosome punctates after apoptosis induction.

We further tested whether final degradation of autophagic cargo inside autophagolysosomes had any effect on vFLIP's inhibition of apoptosis. HeLa-vFLIP stable cells were treated with ammonium chloride at 4, 6, and 8 h after apoptosis induction to prevent pH drop in lysosomes and harvested for Western blot analysis. In HeLa-vFLIP stable cells, a cleavage band of PARP-1 at 89 kDa was observed at 4 and 6 h, and became weaker at 8 h, while in HeLa cells with empty vector, a strong band of PARP-1 at 89 kDa was observed at all these time points (Fig. 16). This result indicates

that inhibition of autophagolysosomes at 4 and 6 h after apoptosis induction had a little effect on vLFIP's anti-apoptotic function. An increase of autophagosome formation at an early time point in cells expressing vFLIP suggested an important role in apoptosis inhibition, while a later time point had less effect. In normal cells, the response of autophagic vacuolization at an early phase was much less observed and does not protect cells from apoptotic death. A similar phenomenon has been observed in other cell types including MCF-7 cells. MCF-7 cells treated with Camptothecin, a chemical inducing intrinsic apoptosis, rapidly underwent apoptosis, while simultaneously triggering an autophagic response in the cells can delay apoptotic death (9). Although the underlying mechanism regardingremains unclear how autophagic vacuolization participates in apoptosis inhibition, it has been hypothesized is that some proteins in apoptosis and autophagy have cross talk.

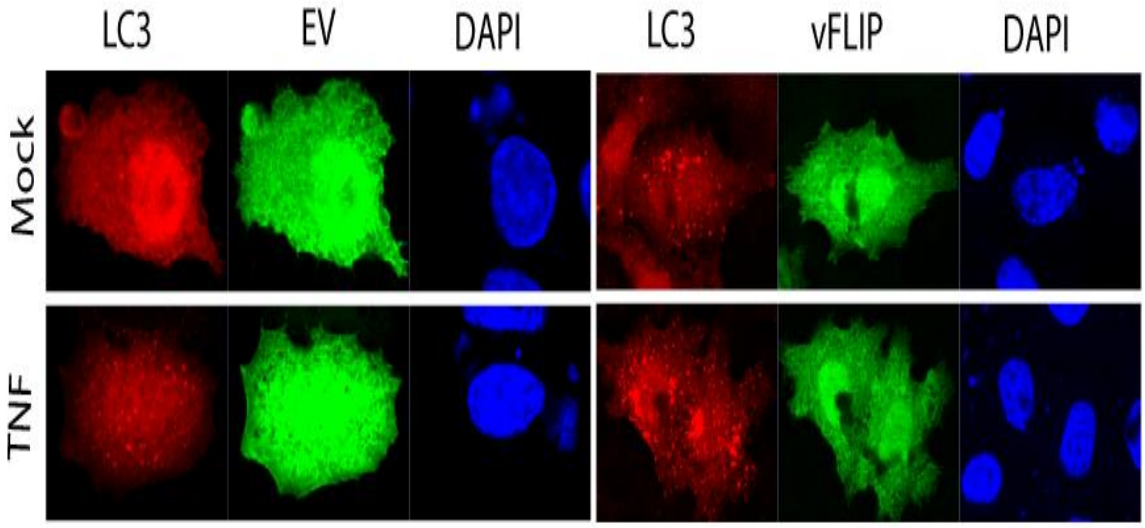

Figure 13. Increased autophagosome formation in HeLa cells after apoptosis induction. RRV vFLIP expression leads to increase of autophagosome punctates in HeLa cells after apoptosis induction. HeLa cells were co-transfected with mCherry-LC3 and VenusN1-vFLIP or empty vector (EV), and on next day, induced with TNF-α and cycloheximide for 3 h. The cells were observed under confocal fluorescence microscopy. Nuclear DNA was counterstained with DAPI. Mock: no apoptosis induction. TNF: at 3 h after apoptosis induction.

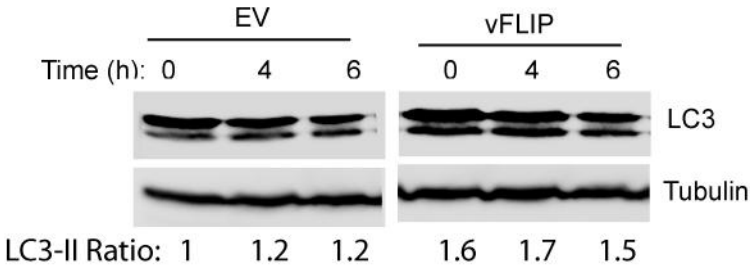

Figure 14. Upregulation of LC3-II in RRV vFLIP expressing cells after apoptosis induction by Western blot analysis. Increase of LC3-II in cells with vFLIP expression after apoptosis induction. HeLa-vFLIP stable and HeLa cells with EV were transfected with CFP-LC3, and, on the next day induced with TNF-α and cycloheximide to undergo apoptosis. The cells were harvested at 0, 4, and 6 h after the induction for Western blot analysis of LC3. Tubulin was blotted for normalization. The relative ratios of LC3-II (the lower band of LC3 image) in comparison with HeLa-EV cells at 0 h after apoptosis induction are shown below the image.

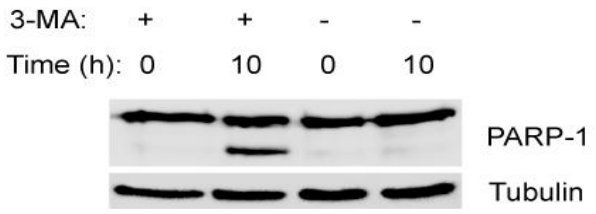

Figure 15. Effect of 3-MA on anti-apoptotic function of RRV vFLIP. 3-MA was added to HeLa-vFLIP stable cells at 1 h before addition of TNF-α and cycloheximide. The cells were harvested at 10 h after TNF-α addition for Western blot analysis of PARP-1 cleavage.

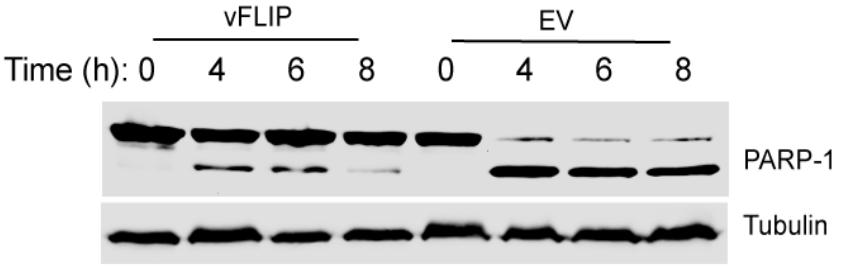

Figure16. Effect of NH4Cl on anti-apoptotic function of RRV vFLIP. NH4Cl was added to HeLa-vFLIP or HeLa-EV cells at 4, 6 and 8 h after apoptosis induction. The cells were harvested at 10 h after TNF-α addition.

4.6 Inhibition of autophagic cell death induced by rapamycin treatment

The above data shows that RRV vFLIP protects cells against apoptosis by enhancing autophagosome formation. In addition to its undisputable role in cell survival in adverse conditions, autophagy can also be induced as a part of cell death that is described as type II programmed cell death (3). Autophagy literally is a defense

mechanism to enhance cell survival. We were interested in RRV vFLIP's role in autophagic cell death. It was reported that cellular and viral FLIPs suppress autophagic cell death by preventing Atg3 from binding and processing LC3. To determine whether RRV vFLIP can also suppress autophagic cell death, we transfected HeLa-LC3 stable cells with VenusN1-vFLIP or empty vector and, on the next day, treated the cells with rapamycin, an mTOR inhibitor, at a final concentration of 4 μM. The cells were harvested for Western blott analysis and confocal microscopy at 0, 6, and 9 h after rapamycin treatment (Fig.17 and 18). A weaker band of LC3-II was observed in cells expressing vFLIP at 6 and 9 h after induction than cells with empty vector. The ratio of LC3-I:LC3-II was decreased from 1.46 at 0 h to 0.87 at 9 h in HeLa cells transfected with empty vector. With the presence of RRV vFLIP, the ratio of LC3-I:LC3-II was slightly increased from 1.26 at 0 h to 1.46 at 9 h. This result indicates that RRV vFLIP inhibits rapamycin-induced autophagy that leads to cell death.

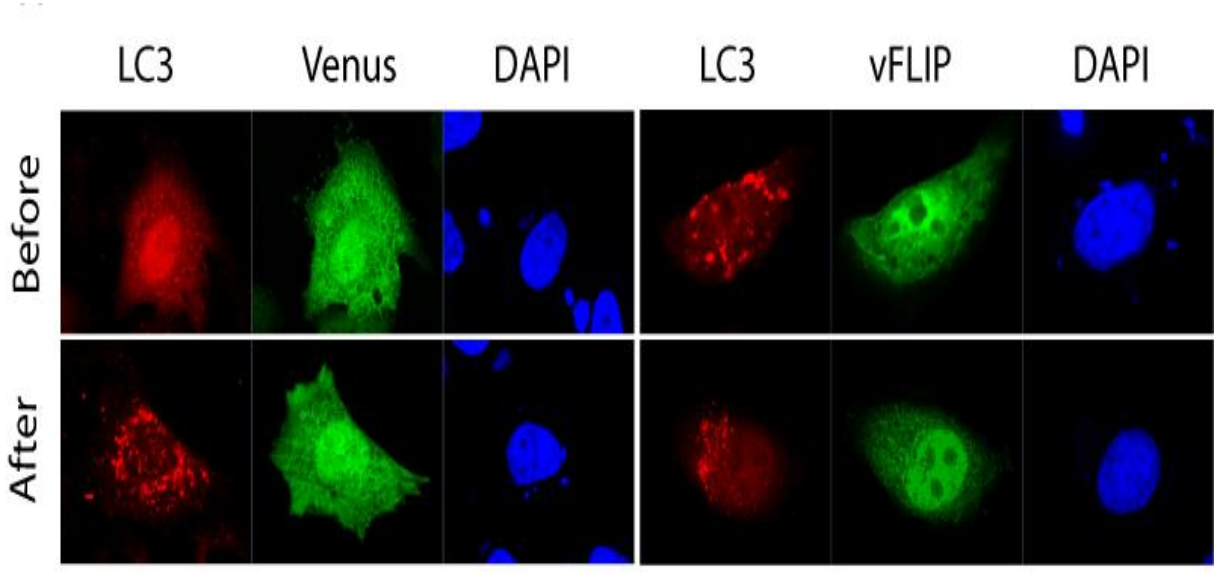

Figure 17. Autophagosome formation in HeLa cells after rapamycin treatment. Expression of vFLIP reduces autophagosome punctates induced by rapamycin. HeLa cells co-transfected with mCherry-LC3 and VenusN1-vFLIP or VenusN1 were treated with rapamycin for 6 h and observed under confocal fluorescence microscopy. Nuclear DNA was counterstained with DAPI. Before: at 0 h of rapamycin treatment. After: at 6 h after rapamycin treatment.

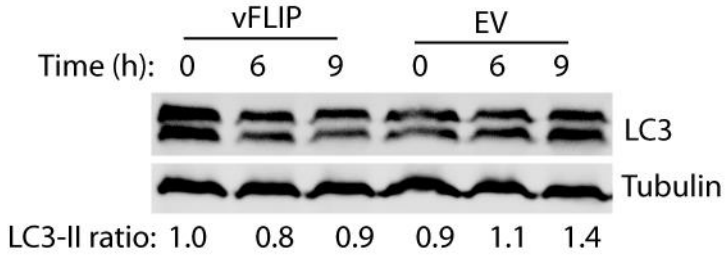

Figure 18. Inhibition of rapamycin-induced autophagy in HeLa cells Reduction of LC3-II in RRV vFLIP expressing. vFLIP reduces LC3-II level induced by rapamycin. HeLa-LC3 stable cells were transfected with either VenusN1-vFLIP or empty vector, and on next day, treated with rapamycin. The cells were harvested at 0, 6, and 9 h after the treatment for Western blotting analysis with LC3 antibody. Tubulin was blotted for normalization. The relative ratios of LC3-II (the lower band of LC3 image) in comparison with HeLa-vFLIP stable cells at 0 h after rapamycin induction are shown below the image.

4.7 Truncated vFLIP proteins lose the roles of the full-length vFLIP on apoptosis and autophagy pathway

Our data above shows that RRV vFLIP inhibits apoptosis by enhancing autophagosome formation and suppresses autophagic cell death to promote cell survival.

To understand whether any specific vFLIP domains might be responsible for these effects, we generated RRV vFLIP deletion constructs and tested their roles in the inhibition of apoptosis and autophagic cell death. RRV ORF71 gene was used as a template to construct three truncation plasmids in VenusN1 vector. Western-blot analysis of whole proteins from cells transfected with these plasmids showed the expression of the three truncated vFLIP proteins (Fig. 19).

HeLa cells transfected with the three vFLIP truncation constructs were treated with TNF-α and cycloheximide to induce apoptosis. The cleavage band of PARP-1 at 89 kDa was obviously observed from cells transfected with each of the three truncated vFLIPs, similar to that from cells transfected with an empty vector or mock-transfected (Fig. 20). The cells transfected with plasmid of full-length vFLIP had no PARP-1 cleavage after apoptotic induction. This result indicates that deletion at either amino- or carboxy-terminus of vFLIP disrupted its function in the inhibition of apoptosis.

To test whether these truncations of vFLIP could inhibit autophagic cell death, we transfected HeLa-LC3 stable cells with individual deletion constructs and treated the cells with rapamycin. The cells were harvested at 6 h after the induction for Western blotting analysis. The intensity of LC3-II bands from cells transfected with the three vFLIP deletion constructs was similar to that from cells mock-transfected (Fig. 21). The LC3-I:LC3-II ratio from all truncations and mock-transfected cells was much lower than that from cells with full length vFLIP and no-induction control. This result suggests that all three vFLIP truncations were unable to suppress rapamycin-induced autophagy development.

Taken together, the full-length vFLIP protein is required to fulfill its function in the inhibition of apoptosis and autophagy. Possibly, the full-length protein might facilitate the proper protein folding, which allows RRV vFLIP to interact with cellular proteins.

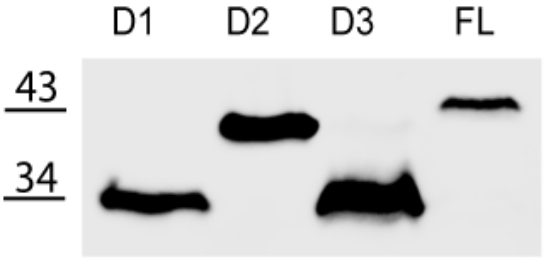

Figure 19. Expression of the truncations of RRV vFLIP protein. Detection of expression of the vFLIP truncations in HEK293 cells by rabbit anti-vFLIP antibody. Molecular weight markers are indicated on the left of image.

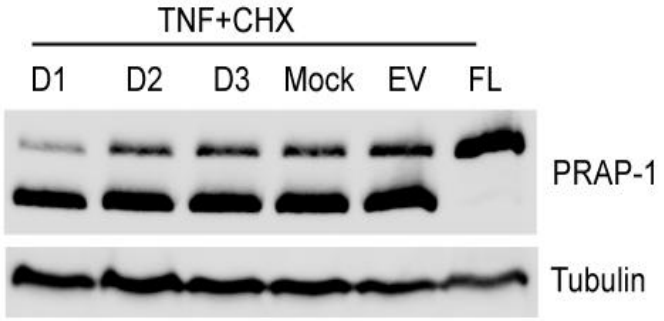

Figure 20. Truncation variants of RRV vFLIP protein are unable to inhibit apoptosis. . Full length vFLIP is needed for inhibition of apoptosis induced by TNF-α and cycloheximide. HeLa cells were transfected with VenusN1-D1, VenusN1-D2, VenusN1-D3, VenusN1-vFLIP (FL), and VenusN1 (EV). The cells were induced with

TNF-α and cycloheximide one day post-transfection to undergo apoptosis, and harvested at 10 h after induction to detect PARP-1 cleavage.

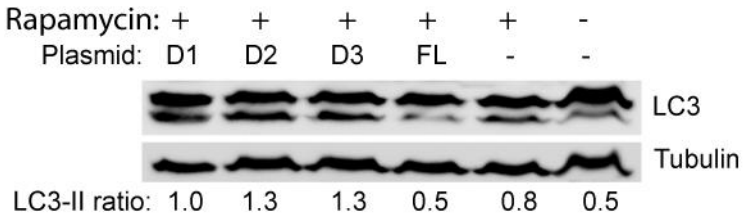

Figure 21. Truncation variants of RRV vFLIP protein unable to inhibit rapamycin-induced autohpagy. HeLa-LC3 cells were transfected with D1, D2, D3, and VenusN1-vFLIP (FL). The cells were treated with 4 μM rapamycin next day, and harvested at 6 h after the treatment. Tubulin was blotted for normalization. The relative ratios of LC3-II (the lower band of LC3 image) in comparison with D1 after rapamycin induction are shown below the image.

4.8 RRV latent infection of BJAB cells protects the cells against apoptosis induction and suppression of vFLIP with siRNA abolishes the protection

Although several cell lines can be infected with RRV, the main target cells of RRV latent infection *in vivo* are B cells (7). To examine autophagy in RRV-infected cells, we used BJAB cells as latent RRV infection occurred in the cells and vFLIP is a latent protein and could play a role during the latent phase of RRV infection. BJAB cells were infected with RRV at 2 MOI and maintained for two weeks in culture. BJAB cells latently infected with RRV (BJAB-RRV) and normal BJAB cells were induced to undergo apoptosis and harvested for Western blot analysis at 2 h after the treatment. The cleaved band of PARP-1 at 89 kDa was strong in BJAB, but much weaker in BJAB-RRV (lane 2 in each image

of Fig 22). To test whether autophagy is needed for the inhibition of apoptosis in BJAB-RRV, we treated the cells with 3-MA for 3 hours prior to apoptosis induction or ammonium chloride at the same time of apoptosis induction. PARP-1 cleavage was highly increased in BJAB-RRV when treated with either 3-MA or ammonium chloride (lane 3 and 4 in the second image of Fig.22). These treatments also increased PARP-1 cleavage in normal BJAB cells (lane 3 and 4 in the first image of Fig. 22), as expected. This result indicates that the anti-apoptotic function coupled with autophagosome formation in RRV-infected BJAB cells corroborates with the data in HeLa cells stably expressing vFLIP. Live cell counting demonstrated that BJAB-RRV had much more live cells than BJAB cells at 6 h after apoptosis induction (Fig. 23), which is consistent with the levels of PARP-1 cleavage in the cells.

To further confirm that the inhibition of apoptosis via antophagy pathway in RRV-infected BJAB cells was due to vFLIP expression, we treated BJAB-RRV cells with a siRNA against vFLIP to knockdown vFLIP expression in the cells. A siRNA against ORF-K9 of KSHV was included as a control. To test the efficacy and specificity of siRNA against vFLIP, HEK293 cells were cotransfected with VenusN1-vFLIP and siRNA against RRV vFLIP or KSHV K9. On the following day, the transfected cells were observed under fluorescence microscope. Fluorescence signal was significantly decreased in the cells cotransfected with VenusN1-vFLIP and siRNA against vFLIP as compared with control (Fig 24). Real-time RT-PCR showed that vFLIP mRNA in BJAB-RRV was reduced significantly after treatment with vFLIP siRNA, while K9 siRNA had no effect (Fig 25). The cells were induced to undergo apoptosis one day after the siRNA transfection. Western blotting analysis showed that PARP-1 cleavage was

increased in BJAB-RRV after treatment with vFLIP siRNA in comparison with the control siRNA to K9 (Fig. 26), indicating that vFLIP is needed for the apoptosis inhibition. Treatment of normal BJAB cells with both siRNAs led to a slight increase in PARP-1 cleavage after apoptosis induction. This result suggests that vFLIP can inhibit apoptosis via autophagy pathway in RRV-infected cells.

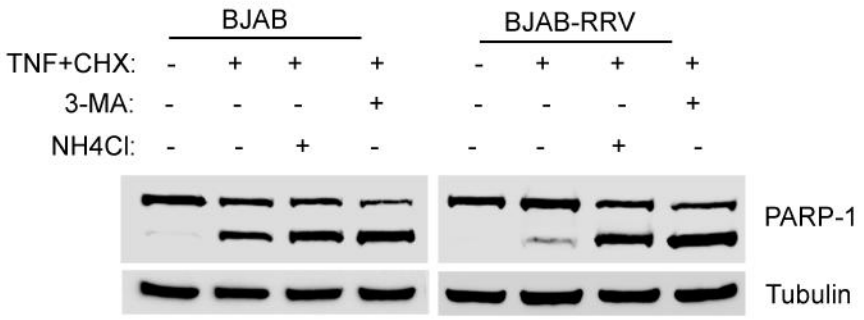

Figure 22 Latent infection of BJAB cells by RRV assists cell survival. RRV latent infection of BJAB cells protects the cells against apoptosis and inhibition of autophagy abolishes the protective effect. BJAB cells latently infected with RRV (BJAB-RRV) were either untreated, treated with 3-MA for 3 hours prior to apoptosis induction by TNF-α and cycloheximide or treated with ammonium chloride at the same time of the apoptosis induction. The cells were harvested at 2 hours post-apoptosis induction for Western blot analysis of PARP-1 cleavage. Similar treatment of uninfected BJAB cells was included as a control

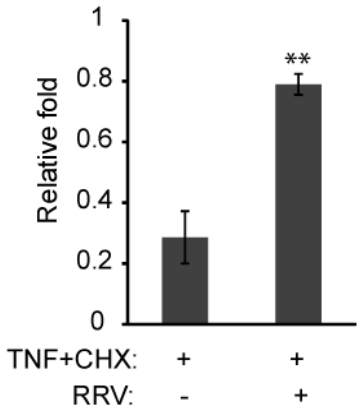

Figure 23. Cell viability assay of BJAB and BJAB-RRV cells after apoptosis induction. Relative folds in comparison with uninfected BJAB cells at 0 h are shown. Significant differences between BJAB and BJAB-RRV cells after apoptosis induction are denoted by "**", which indicates $P < 0.01$.

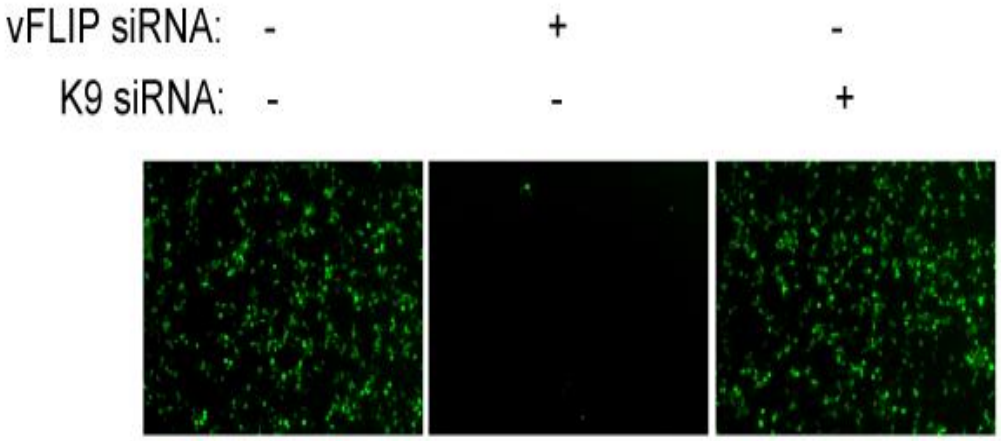

Figure 24 siRNA mediated suppression of vFLIP expression in HEK293 cells transiently transfected with VenusN1-vFLIP. The cells were transfected with VenusN1-vFLIP plasmid. Transfection of the cells with siRNA against vFLIP or K9 was done at the same time of plasmid transfection. Observation under fluorescence

microscopy was conducted one day post-tranfection. The siRNA against KSHV K9 was included as a negative control.

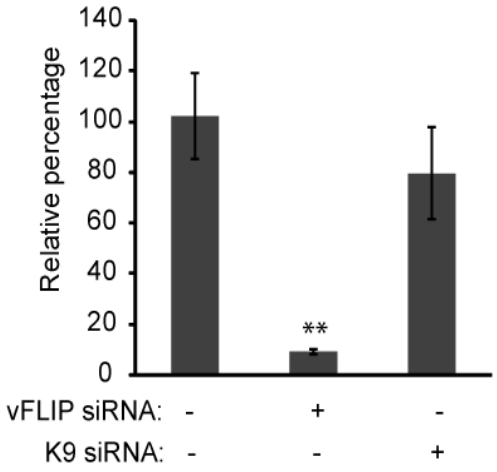

Figure 25 siRNA-mediated suppression vFLIP expression in RRV-infected BJAB cells. BJAB cells latently infected with RRV were transfected with a siRNA against vFLIP. A siRNA against KSHV K9 was included as a negative control. The cells were harvested at 24 h after the transfection. Real-time RT-PCR was conducted to assess vFLIP transcript level. Relative percentages in comparison with mock-treated control are shown. Significant differences between siRNA-treated and mock-treated BJAB-RRV cells are denoted by "**", which indicates $P < 0.01$.

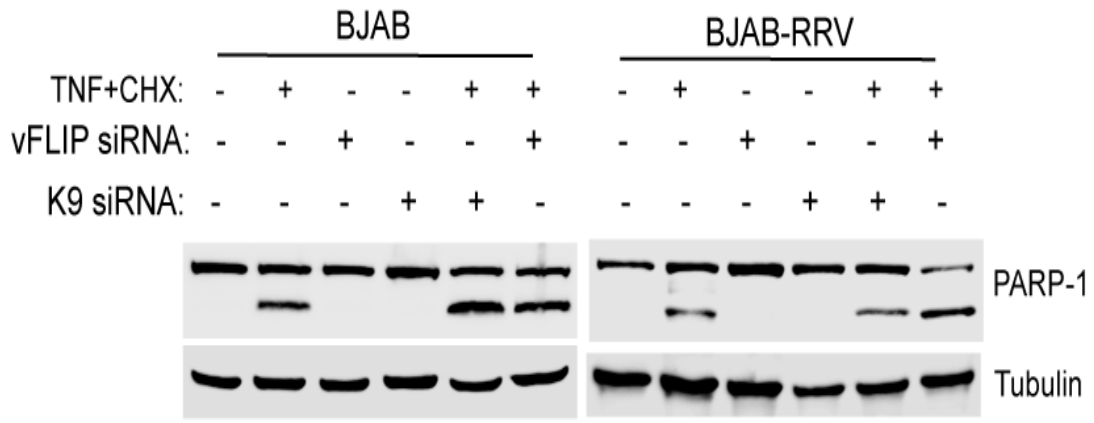

Figure 26 Suppression of RRV vFLIP gene expression in BJAB-RRV cells leads to loss of the capability of anti-apoptosis function. BJAB cells latently infected with RRV were transfected with siRNA against vFLIP at 15 hours before apoptosis induction. siRNA against KSHV ORFK9 was included as a control. Treatment of uninfected BJAB cells was included as a control. The cells were harvested at 2 hours after treatment with TNF-α and cycloheximide for Western blot analysis of PARP-1 cleavage.

Chapter 5: Discussion

Several γ-herpesviruses contain vFLIP genes. However, not all of the vFLIPs have similar functions. In this study, we found RRV vFLIP has anti-apoptosis function, similar to KSHV vFLIP. However, unlike KSHV vFLIP, RRV vFLIP cannot activate NF-κB as shown by the NF-κB reporter assay and nuclear translocation experiment. NF-κB is a pluripotent transcription factor that plays important roles in several cellular signaling pathways including apoptosis, cell adhesion, proliferation, innate- and adaptive-immune responses, inflammation, stress response, and tissue remodeling (79). The gene expression in these pathways is coherently coupled with other transcription factors and cellular signals as well. Thus, the anti-apoptosis function of RRV vFLIP is not due to NF-κB signaling. Instead, our data show that RRV vFLIP inhibit apoptosis via enhancement of autophagy to promote cell survival, while autophagic cell death was inhibited.

We expressed Venus-vFLIP fusion protein in this study. We could not detect vFLIP when vFLIP is expressed alone or with short tag, which indicates that the protein is very unstable or the turnover rate is high in the cells. We tried MG132, a specific and potent proteosome inhibitor, to the cells after transfection with the vFLIP expression plasmids and did not detect any vFLIP either, indicating the protein was possibly not degraded by the ubiquitin pathway if it was due to rapid degradation. Similarly, in RRV-infected RhF or BJAB cells, the protein is also below detection level. It appears that the fusion with Venus stabilizes the protein. In transiently transfected cells, the protein locates in the nucleus and cytoplasm. The presence of the protein in cytoplasm is consistent with its function of anti-apoptosis, however, its presence in the nucleus might be linked to unknown functions.

We used a combination of TNF-α and cycloheximide to induce apoptosis. Either one of them could not induce apoptosis at the concentration used in this study. The cycloheximide sensitizes the cells to undergo apoptosis induced by TNF-α. The cleavage of procaspase 9 indicates that the intrinsic pathway was activated by the apoptosis induction. The caspase activity assay result is consistent with this observation. We speculate that the activation of intrinsic pathway might be due the combination of the two compounds or detection time after the induction. The second point is less likely as we tested caspase activity in several time points after the induction and a similar trend was observed. Our finding of up-regulation of MnSOD in HeLa-vFLIP stable cells is consistent with the activation of intrinsic pathway. MnSOD contributes to suppression of apoptosis by reducing accumulation of intracellular superoxide to enhance cell survival (103).

Whereas an increase of MnSOD after KSHV infection is linked to NF-κB activation, we found up-regulated MnSOD gene expression in HeLa cells with vFLIP expression in the absence of NF-κB activation. This finding suggests that NF-κB pathway may not be the only factor that controls MnSOD expression, but other transcription factors could also be involved in the regulation of this gene as well. It was reported that p53 responds to physiological stress by stimulating redox-controlling genes to reduce ROS level. The increase of MnSOD transcript in HeLa cells with vFLIP expression suggests that RRV vFLIP might employ p53 or other transcription factors (38).

Expression of vFLIP in HeLa cells enhanced cell survival under starved condition. HBSS was added to the cells after growth medium was removed. As nutrient

deprivation induces autophagy, extension of cell survival of HeLa-vFLIP cells indicates that vFLIP suppresses autophagy. Autophagy is a multi-step process beginning with the formation of autophagosome-cytoplasmic vesicles that have a double membrane and contain cytoplasmic cargo, fusion of autophagosomes with lysosomes to become autophagolysosomes, and degradation of contents in the autophagolysosomes. Enhancement of cell survival under starved condition in HeLa-vFLIP stable cells prompted us to determine autophagy before and after apoptosis induction. Interestingly, we found that autophagosome formation was increased in HeLa-vFLIP stable cells at early time points after apoptosis induction. When autophagy was inhibited at either early autophagosome formation by 3-MA or late autophagosome degradation step by ammonium chloride, vFLIP could no longer protect the cells against apoptosis. The addition of ammonium chloride at 8 h after apoptosis induction to inhibit autophagosome degradation step had less effect on the function of RRV vFLIP in inhibition of apoptosis than earlier time points. The apoptosis induction in HeLa cells is much more efficient in the presence of ammonium chloride.This result suggests that autophagy at early time points after apoptosis induction is essential for RRV vFLIP to protect the cells from apoptosis. Our findings are consistent with previous publications that explored both apoptosis and autophagy pathways. For example, two colon-cancer-derived cell lines, colon 26 and HT29 significantly underwent apoptosis after the combination treatment of 3-MA to inhibit autophagy and 5-FU to induce apoptosis (62). Likewise, MCF-7, a breast cancer cell line, delayed apoptotic death following autophagy induction by nutrient starvation. Inhibition of the expression of Beclin 1 and Atg7 stimulates apoptosis in DNA-damaged MCF-7 cells (1).

Noticeably, LC3-II was present at a relatively higher level in cells with RRV vFLIP expression than control cells even without apoptosis induction. We speculate that RRV vFLIP induces a basal level of autophagy to promptly respond to stress signals in order to promote cell survival. The accumulation of autophagosomes in HeLa-vFLIP stable cells is possibly due to increased formation or slower turnover rate. The data in Fig. 13 indicates more autophagosome formation might account for the increased level. It has been reported that autophagy in MCF-7 cells due to nutrient starvation delays apoptotic death induced by camptothecin, a DNA-damaging compound (1). In addition, treatment with autophagy inhibitors increased mitochondrial depolarization and caspase-9 activity, resulting in apoptosis. RRV vFLIP also employs autophagy during early time points after apoptosis induction to protect cells against apoptosis.

Although autophagy is considered a mechanism to enhance cell survival in adverse conditions, it is also classified as type II programmed cell death due to accumulation of autophagosomes in the cytoplasm under pathological conditions. It was reported that FLIP inhibits autophagic cell death induced by rapamycin by preventing Atg3 from binding and processing LC3 (58). The function of RRV vFLIP in the inhibition of autopahgic cell death is consistent with other vFLIPs described in the previous report. The autophagosome accumulation in HeLa-vFLIP stable cells at 6 and 9 h after rapamycin treatment was much lower than control cells. This indicates that autophagosome formation was inhibited, possibly by preventing Atg3 from binding LC3 as other vFLIPs. The enhancement of autophagosomes in HeLa-vFLIP stable cells after apoptosis induction indicates that a different mechanism is activated because vFLIP binding Atg3 inhibits autophagy. How the RRV vFLIP activates other mechanisms while

avoiding the effect of interaction with Atg3 is not known. We hypothesize that RRV vFLIP activates autophagy through interaction with a cellular factor activated by apoptosis induction. The up-regulation of MnSOD in HeLa-vFLIP stable cells is consistent with this hypothesis.

The RRV vFLIP deletion mutants were established to determine their functional domains in the inhibition of apoptosis and autophagy. All of the truncated proteins failed to perform the functions, which implies that full-length vFLIP protein is required for the inhibition. However, small peptides containing DED1 α2 helix or DED2 α4 helix of FLIP are able to bind with FLIP and Atg3 and effectively interfere with Atg3-FLIP interaction, which results in autophagic cell death. We did not observe the induction of autophagic cell death in cells expressing the truncated vFLIP in our study. As we could not detect the expression of RRV vFLIP alone we used fusion protein with GFP was used in our study. It would be possible that GFP might interfere with the function of the RRV vFLIP truncation fragments though the possibility is remote.

Since B cells are targeted by natural infection of RRV, BJAB cells were latently infected with RRV to verify the observation in HeLa cells with vFLIP expression. It has been reported that RRV latently and persistently infected immortalized B-cell lines (7). The expression of the cluster of RRV latent genes during the latent phase was verified by real-time RT-PCR. However, RRV vFLIP protein in BJAB cells with RRV latent infection was below detection level, indicating its short half life. Interestingly, BJAB cells with RRV latent infection resisted apoptosis induction. Moreover, when autophagy was inhibited with 3-MA or ammonium chloride, the BJAB cells with RRV infection lost the ability to escape from apoptosis. Knockdown of vFLIP expression with siRNA leads

to loss of the anti-apoptosis effect in BJAB-RRV, which indicates that vFLIP is possibly the viral gene accounting for the anti-apoptosis function. The data in BJAB cells is consistent with the observation in HeLa cells. There are other genes in RRV such as vBcl-2, which inhibits autophagy and apoptosis. Our data indicates that these other genes might not involve in the protection of cells from apoptosis induction via autophagy pathway.

The exact mechanisms for RRV vFLIP to enhance autophagosome formation during early apoptosis remain unclear. Autophagy pathway is thought to contribute in cell survival by cross talking with apoptosis pathway. Mitochondria membrane permeabilization and cytochrome C release are a critical step during apoptotic cell death. However, when the damage in mitochondria is below the threshold required for apoptosis, the damaged mitochondria will be sequestered in autophagosomes. The autophagic process provides a source of metabolic energy in the form of ATP from damaged organelles and long-lived proteins. The dual effects of RRV vFLIP to enhance autophagy in apoptosis induction and inhibit rapamycin-induced autophagic cell death provide a great benefit to promote cell survival and prevent cell death. Further study on interaction of RRV vFLIP with cellular factors is warranted and may yield informative data that can be extrapolated to the management of KSHV-associated maligancies.

Bibliography

1. Abedin, M. J., D. Wang, M. A. McDonnell, U. Lehmann, and A. Kelekar. 2007. Autophagy delays apoptotic death in breast cancer cells following DNA damage. Cell death and differentiation 14:500-510.
2. Alexander, L., L. Denekamp, A. Knapp, M. R. Auerbach, B. Damania, and R. C. Desrosiers. 2000. The primary sequence of rhesus monkey rhadinovirus isolate 26-95: sequence similarities to Kaposi's sarcoma-associated herpesvirus and rhesus monkey rhadinovirus isolate 17577. Journal of virology 74:3388-3398.
3. Baehrecke, E. H. 2005. Autophagy: dual roles in life and death? Nature reviews. Molecular cell biology 6:505-510.
4. Baehrecke, E. H. 2002. How death shapes life during development. Nature reviews. Molecular cell biology 3:779-787.
5. Barton, E., P. Mandal, and S. H. Speck. 2011. Pathogenesis and host control of gammaherpesviruses: lessons from the mouse. Annual review of immunology 29:351-397.
6. Bertin, J., R. C. Armstrong, S. Ottilie, D. A. Martin, Y. Wang, S. Banks, G. H. Wang, T. G. Senkevich, E. S. Alnemri, B. Moss, M. J. Lenardo, K. J. Tomaselli, and J. I. Cohen. 1997. Death effector domain-containing herpesvirus and poxvirus proteins inhibit both Fas- and TNFR1-induced apoptosis. Proceedings of the National Academy of Sciences of the United States of America 94:1172-1176.
7. Bilello, J. P., S. M. Lang, F. Wang, J. C. Aster, and R. C. Desrosiers. 2006. Infection and persistence of rhesus monkey rhadinovirus in immortalized B-cell lines. J Virol 80:3644-3649.
8. Boldin, M. P., E. E. Varfolomeev, Z. Pancer, I. L. Mett, J. H. Camonis, and D. Wallach. 1995. A novel protein that interacts with the death domain of Fas/APO1 contains a sequence motif related to the death domain. The Journal of biological chemistry 270:7795-7798.
9. Bursch, W., A. Ellinger, H. Kienzl, L. Torok, S. Pandey, M. Sikorska, R. Walker, and R. S. Hermann. 1996. Active cell death induced by the anti-estrogens tamoxifen and ICI 164 384 in human mammary carcinoma cells (MCF-7) in culture: the role of autophagy. Carcinogenesis 17:1595-1607.
10. Chang, H., L. M. Wachtman, C. B. Pearson, J. S. Lee, H. R. Lee, S. H. Lee, J. Vieira, K. G. Mansfield, and J. U. Jung. 2009. Non-human primate model of Kaposi's sarcoma-associated herpesvirus infection. PLoS pathogens 5:e1000606.
11. Chaudhary, P. M., A. Jasmin, M. T. Eby, and L. Hood. 1999. Modulation of the NF-kappa B pathway by virally encoded death effector domains-containing proteins. Oncogene 18:5738-5746.
12. Chinnaiyan, A. M., K. O'Rourke, M. Tewari, and V. M. Dixit. 1995. FADD, a novel death domain-containing protein, interacts with the death domain of Fas and initiates apoptosis. Cell 81:505-512.
13. Cleary, M. L., S. D. Smith, and J. Sklar. 1986. Cloning and structural analysis of cDNAs for bcl-2 and a hybrid bcl-2/immunoglobulin transcript resulting from the t(14;18) translocation. Cell 47:19-28.
14. Compton, T. 1993. An immortalized human fibroblast cell line is permissive for human cytomegalovirus infection. Journal of virology 67:3644-3648.

15. Damania, B., and R. C. Desrosiers. 2001. Simian homologues of human herpesvirus 8. Philosophical transactions of the Royal Society of London. Series B, Biological sciences 356:535-543.
16. Davison, A. J., R. Eberle, B. Ehlers, G. S. Hayward, D. J. McGeoch, A. C. Minson, P. E. Pellett, B. Roizman, M. J. Studdert, and E. Thiry. 2009. The order Herpesvirales. Arch Virol 154:171-177.
17. Degenhardt, K., R. Mathew, B. Beaudoin, K. Bray, D. Anderson, G. Chen, C. Mukherjee, Y. Shi, C. Gelinas, Y. Fan, D. A. Nelson, S. Jin, and E. White. 2006. Autophagy promotes tumor cell survival and restricts necrosis, inflammation, and tumorigenesis. Cancer cell 10:51-64.
18. Deretic, V. 2010. Autophagy in infection. Current opinion in cell biology 22:252-262.
19. Desrosiers, R. C., V. G. Sasseville, S. C. Czajak, X. Zhang, K. G. Mansfield, A. Kaur, R. P. Johnson, A. A. Lackner, and J. U. Jung. 1997. A herpesvirus of rhesus monkeys related to the human Kaposi's sarcoma-associated herpesvirus. J Virol 71:9764-9769.
20. DeWire, S. M., M. A. McVoy, and B. Damania. 2002. Kinetics of expression of rhesus monkey rhadinovirus (RRV) and identification and characterization of a polycistronic transcript encoding the RRV Orf50/Rta, RRV R8, and R8.1 genes. J Virol 76:9819-9831.
21. DeWire, S. M., M. A. McVoy, and B. Damania. 2002. Kinetics of expression of rhesus monkey rhadinovirus (RRV) and identification and characterization of a polycistronic transcript encoding the RRV Orf50/Rta, RRV R8, and R8.1 genes. Journal of virology 76:9819-9831.
22. DeWire, S. M., E. S. Money, S. P. Krall, and B. Damania. 2003. Rhesus monkey rhadinovirus (RRV): construction of a RRV-GFP recombinant virus and development of assays to assess viral replication. Virology 312:122-134.
23. Dimitrov, T., P. Krajcsi, T. W. Hermiston, A. E. Tollefson, M. Hannink, and W. S. Wold. 1997. Adenovirus E3-10.4K/14.5K protein complex inhibits tumor necrosis factor-induced translocation of cytosolic phospholipase A2 to membranes. Journal of virology 71:2830-2837.
24. Dittmer, D., C. Stoddart, R. Renne, V. Linquist-Stepps, M. E. Moreno, C. Bare, J. M. McCune, and D. Ganem. 1999. Experimental transmission of Kaposi's sarcoma-associated herpesvirus (KSHV/HHV-8) to SCID-hu Thy/Liv mice. The Journal of experimental medicine 190:1857-1868.
25. Dittmer, D. P., C. M. Gonzalez, W. Vahrson, S. M. DeWire, R. Hines-Boykin, and B. Damania. 2005. Whole-genome transcription profiling of rhesus monkey rhadinovirus. J Virol 79:8637-8650.
26. Efklidou, S., R. Bailey, N. Field, M. Noursadeghi, and M. K. Collins. 2008. vFLIP from KSHV inhibits anoikis of primary endothelial cells. Journal of cell science 121:450-457.
27. Erlich, S., L. Mizrachy, O. Segev, L. Lindenboim, O. Zmira, S. Adi-Harel, J. A. Hirsch, R. Stein, and R. Pinkas-Kramarski. 2007. Differential interactions between Beclin 1 and Bcl-2 family members. Autophagy 3:561-568.
28. Fan, T. J., L. H. Han, R. S. Cong, and J. Liang. 2005. Caspase family proteases and apoptosis. Acta biochimica et biophysica Sinica 37:719-727.

29. Fedorov, L. M., C. Schmittwolf, K. Amann, W. H. Thomas, A. M. Muller, H. Schubert, J. Domen, and B. Kneitz. 2006. Renal failure causes early death of bcl-2 deficient mice. Mechanisms of ageing and development 127:600-609.
30. Field, N., W. Low, M. Daniels, S. Howell, L. Daviet, C. Boshoff, and M. Collins. 2003. KSHV vFLIP binds to IKK-gamma to activate IKK. J Cell Sci 116:3721-3728.
31. Flemington, E. K. 2001. Herpesvirus lytic replication and the cell cycle: arresting new developments. Journal of virology 75:4475-4481.
32. Fujimura, M., Y. Morita-Fujimura, M. Kawase, J. C. Copin, B. Calagui, C. J. Epstein, and P. H. Chan. 1999. Manganese superoxide dismutase mediates the early release of mitochondrial cytochrome C and subsequent DNA fragmentation after permanent focal cerebral ischemia in mice. The Journal of neuroscience : the official journal of the Society for Neuroscience 19:3414-3422.
33. Garvey, T., J. Bertin, R. Siegel, M. Lenardo, and J. Cohen. 2002. The death effector domains (DEDs) of the molluscum contagiosum virus MC159 v-FLIP protein are not functionally interchangeable with each other or with the DEDs of caspase-8. Virology 300:217-225.
34. Hars, E. S., H. Qi, A. G. Ryazanov, S. Jin, L. Cai, C. Hu, and L. F. Liu. 2007. Autophagy regulates ageing in C. elegans. Autophagy 3:93-95.
35. Hoyer-Hansen, M., L. Bastholm, P. Szyniarowski, M. Campanella, G. Szabadkai, T. Farkas, K. Bianchi, N. Fehrenbacher, F. Elling, R. Rizzuto, I. S. Mathiasen, and M. Jaattela. 2007. Control of macroautophagy by calcium, calmodulin-dependent kinase kinase-beta, and Bcl-2. Molecular cell 25:193-205.
36. Hu, S., C. Vincenz, M. Buller, and V. M. Dixit. 1997. A novel family of viral death effector domain-containing molecules that inhibit both CD-95- and tumor necrosis factor receptor-1-induced apoptosis. J Biol Chem 272:9621-9624.
37. Hubbard, S., N. A. Darmani, G. R. Thrush, D. Dey, L. Burnham, J. M. Thompson, K. Jones, and V. Tiwari. 2010. Zebrafish-encoded 3-O-sulfotransferase-3 isoform mediates herpes simplex virus type 1 entry and spread. Zebrafish 7:181-187.
38. Hussain, S. P., P. Amstad, P. He, A. Robles, S. Lupold, I. Kaneko, M. Ichimiya, S. Sengupta, L. Mechanic, S. Okamura, L. J. Hofseth, M. Moake, M. Nagashima, K. S. Forrester, and C. C. Harris. 2004. p53-induced up-regulation of MnSOD and GPx but not catalase increases oxidative stress and apoptosis. Cancer research 64:2350-2356.
39. Irmler, M., M. Thome, M. Hahne, P. Schneider, K. Hofmann, V. Steiner, J. L. Bodmer, M. Schroter, K. Burns, C. Mattmann, D. Rimoldi, L. E. French, and J. Tschopp. 1997. Inhibition of death receptor signals by cellular FLIP. Nature 388:190-195.
40. Janz, A., M. Oezel, C. Kurzeder, J. Mautner, D. Pich, M. Kost, W. Hammerschmidt, and H. J. Delecluse. 2000. Infectious Epstein-Barr virus lacking major glycoprotein BLLF1 (gp350/220) demonstrates the existence of additional viral ligands. Journal of virology 74:10142-10152.
41. Kang, C., Y. J. You, and L. Avery. 2007. Dual roles of autophagy in the survival of Caenorhabditis elegans during starvation. Genes & development 21:2161-2171.

42. Kannan, H., S. Fan, D. Patel, I. Bossis, and Y. J. Zhang. 2009. The hepatitis E virus open reading frame 3 product interacts with microtubules and interferes with their dynamics. Journal of virology 83:6375-6382.
43. Karbowski, M., K. L. Norris, M. M. Cleland, S. Y. Jeong, and R. J. Youle. 2006. Role of Bax and Bak in mitochondrial morphogenesis. Nature 443:658-662.
44. Kelekar, A., and C. B. Thompson. 1998. Bcl-2-family proteins: the role of the BH3 domain in apoptosis. Trends in cell biology 8:324-330.
45. Kerr, J. F., A. H. Wyllie, and A. R. Currie. 1972. Apoptosis: a basic biological phenomenon with wide-ranging implications in tissue kinetics. British journal of cancer 26:239-257.
46. Kirchoff, V., S. Wong, J. S. St, and G. S. Pari. 2002. Generation of a life-expanded rhesus monkey fibroblast cell line for the growth of rhesus rhadinovirus (RRV). Archives of virology 147:321-333.
47. Klionsky, D. J. 2007. Autophagy: from phenomenology to molecular understanding in less than a decade. Nature reviews. Molecular cell biology 8:931-937.
48. Klionsky, D. J., H. Abeliovich, P. Agostinis, D. K. Agrawal, G. Aliev, D. S. Askew, M. Baba, E. H. Baehrecke, B. A. Bahr, A. Ballabio, B. A. Bamber, D. C. Bassham, E. Bergamini, X. Bi, M. Biard-Piechaczyk, J. S. Blum, D. E. Bredesen, J. L. Brodsky, J. H. Brumell, U. T. Brunk, W. Bursch, N. Camougrand, E. Cebollero, F. Cecconi, Y. Chen, L. S. Chin, A. Choi, C. T. Chu, J. Chung, P. G. Clarke, R. S. Clark, S. G. Clarke, C. Clave, J. L. Cleveland, P. Codogno, M. I. Colombo, A. Coto-Montes, J. M. Cregg, A. M. Cuervo, J. Debnath, F. Demarchi, P. B. Dennis, P. A. Dennis, V. Deretic, R. J. Devenish, F. Di Sano, J. F. Dice, M. Difiglia, S. Dinesh-Kumar, C. W. Distelhorst, M. Djavaheri-Mergny, F. C. Dorsey, W. Droge, M. Dron, W. A. Dunn, Jr., M. Duszenko, N. T. Eissa, Z. Elazar, A. Esclatine, E. L. Eskelinen, L. Fesus, K. D. Finley, J. M. Fuentes, J. Fueyo, K. Fujisaki, B. Galliot, F. B. Gao, D. A. Gewirtz, S. B. Gibson, A. Gohla, A. L. Goldberg, R. Gonzalez, C. Gonzalez-Estevez, S. Gorski, R. A. Gottlieb, D. Haussinger, Y. W. He, K. Heidenreich, J. A. Hill, M. Hoyer-Hansen, X. Hu, W. P. Huang, A. Iwasaki, M. Jaattela, W. T. Jackson, X. Jiang, S. Jin, T. Johansen, J. U. Jung, M. Kadowaki, C. Kang, A. Kelekar, D. H. Kessel, J. A. Kiel, H. P. Kim, A. Kimchi, T. J. Kinsella, K. Kiselyov, K. Kitamoto, E. Knecht, et al. 2008. Guidelines for the use and interpretation of assays for monitoring autophagy in higher eukaryotes. Autophagy 4:151-175.
49. Klionsky, D. J., J. M. Cregg, W. A. Dunn, Jr., S. D. Emr, Y. Sakai, I. V. Sandoval, A. Sibirny, S. Subramani, M. Thumm, M. Veenhuis, and Y. Ohsumi. 2003. A unified nomenclature for yeast autophagy-related genes. Developmental cell 5:539-545.
50. Knappe, A., M. Thurau, H. Niphuis, C. Hiller, S. Wittmann, E. M. Kuhn, B. Rosenwirth, B. Fleckenstein, J. Heeney, and H. Fickenscher. 1998. T-cell lymphoma caused by herpesvirus saimiri C488 independently of ie14/vsag, a viral gene with superantigen homology. Journal of virology 72:3469-3471.
51. Kondo, Y., and S. Kondo. 2006. Autophagy and cancer therapy. Autophagy 2:85-90.

52. Kopitz, J., G. O. Kisen, P. B. Gordon, P. Bohley, and P. O. Seglen. 1990. Nonselective autophagy of cytosolic enzymes by isolated rat hepatocytes. The Journal of cell biology 111:941-953.
53. Kraft, M. S., G. Henning, H. Fickenscher, D. Lengenfelder, J. Tschopp, B. Fleckenstein, and E. Meinl. 1998. Herpesvirus saimiri transforms human T-cell clones to stable growth without inducing resistance to apoptosis. Journal of virology 72:3138-3145.
54. Lacoste, V., P. Mauclere, G. Dubreuil, J. Lewis, M. C. Georges-Courbot, and A. Gessain. 2001. A novel gamma 2-herpesvirus of the Rhadinovirus 2 lineage in chimpanzees. Genome Res 11:1511-1519.
55. Lamkanfi, M., N. Festjens, W. Declercq, T. Vanden Berghe, and P. Vandenabeele. 2007. Caspases in cell survival, proliferation and differentiation. Cell death and differentiation 14:44-55.
56. Launay, S., O. Hermine, M. Fontenay, G. Kroemer, E. Solary, and C. Garrido. 2005. Vital functions for lethal caspases. Oncogene 24:5137-5148.
57. Lee, C. Y., E. A. Clough, P. Yellon, T. M. Teslovich, D. A. Stephan, and E. H. Baehrecke. 2003. Genome-wide analyses of steroid- and radiation-triggered programmed cell death in Drosophila. Current biology : CB 13:350-357.
58. Lee, J. S., Q. Li, J. Y. Lee, S. H. Lee, J. H. Jeong, H. R. Lee, H. Chang, F. C. Zhou, S. J. Gao, C. Liang, and J. U. Jung. 2009. FLIP-mediated autophagy regulation in cell death control. Nat Cell Biol 11:1355-1362.
59. Levine, B., and G. Kroemer. 2008. Autophagy in the pathogenesis of disease. Cell 132:27-42.
60. Li, A., O. Ojogho, and A. Escher. 2006. Saving death: apoptosis for intervention in transplantation and autoimmunity. Clinical & developmental immunology 13:273-282.
61. Li, F. Y., P. D. Jeffrey, J. W. Yu, and Y. Shi. 2006. Crystal structure of a viral FLIP: insights into FLIP-mediated inhibition of death receptor signaling. The Journal of biological chemistry 281:2960-2968.
62. Li, J., N. Hou, A. Faried, S. Tsutsumi, T. Takeuchi, and H. Kuwano. 2009. Inhibition of autophagy by 3-MA enhances the effect of 5-FU-induced apoptosis in colon cancer cells. Annals of surgical oncology 16:761-771.
63. Maiuri, M. C., G. Le Toumelin, A. Criollo, J. C. Rain, F. Gautier, P. Juin, E. Tasdemir, G. Pierron, K. Troulinaki, N. Tavernarakis, J. A. Hickman, O. Geneste, and G. Kroemer. 2007. Functional and physical interaction between Bcl-X(L) and a BH3-like domain in Beclin-1. The EMBO journal 26:2527-2539.
64. Mansfield, K. G., S. V. Westmoreland, C. D. DeBakker, S. Czajak, A. A. Lackner, and R. C. Desrosiers. 1999. Experimental infection of rhesus and pig-tailed macaques with macaque rhadinoviruses. Journal of virology 73:10320-10328.
65. Mavrakis, M., J. Lippincott-Schwartz, C. A. Stratakis, and I. Bossis. 2007. mTOR kinase and the regulatory subunit of protein kinase A (PRKAR1A) spatially and functionally interact during autophagosome maturation. Autophagy 3:151-153.
66. McCord, J. M., and I. Fridovich. 1988. Superoxide dismutase: the first twenty years (1968-1988). Free radical biology & medicine 5:363-369.

67. Melendez, A., Z. Talloczy, M. Seaman, E. L. Eskelinen, D. H. Hall, and B. Levine. 2003. Autophagy genes are essential for dauer development and life-span extension in C. elegans. Science 301:1387-1391.
68. Mesri, E. A., E. Cesarman, and C. Boshoff. 2010. Kaposi's sarcoma and its associated herpesvirus. Nature reviews. Cancer 10:707-719.
69. Mills, K. R., M. Reginato, J. Debnath, B. Queenan, and J. S. Brugge. 2004. Tumor necrosis factor-related apoptosis-inducing ligand (TRAIL) is required for induction of autophagy during lumen formation in vitro. Proceedings of the National Academy of Sciences of the United States of America 101:3438-3443.
70. Montgomery, R. I., M. S. Warner, B. J. Lum, and P. G. Spear. 1996. Herpes simplex virus-1 entry into cells mediated by a novel member of the TNF/NGF receptor family. Cell 87:427-436.
71. Mudhakir, D., and H. Harashima. 2009. Learning from the viral journey: how to enter cells and how to overcome intracellular barriers to reach the nucleus. The AAPS journal 11:65-77.
72. Muzio, M., A. M. Chinnaiyan, F. C. Kischkel, K. O'Rourke, A. Shevchenko, J. Ni, C. Scaffidi, J. D. Bretz, M. Zhang, R. Gentz, M. Mann, P. H. Krammer, M. E. Peter, and V. M. Dixit. 1996. FLICE, a novel FADD-homologous ICE/CED-3-like protease, is recruited to the CD95 (Fas/APO-1) death--inducing signaling complex. Cell 85:817-827.
73. Nicholas, J. 2000. Evolutionary aspects of oncogenic herpesviruses. Molecular pathology : MP 53:222-237.
74. Nuver, J., M. F. Lutke Holzik, M. van Zweeden, H. J. Hoekstra, C. Meijer, A. J. Suurmeijer, H. J. Groen, R. M. Hofstra, W. J. Sluiter, H. Groen, D. T. Sleijfer, and J. A. Gietema. 2005. Genetic variation in the bleomycin hydrolase gene and bleomycin-induced pulmonary toxicity in germ cell cancer patients. Pharmacogenetics and genomics 15:399-405.
75. O'Connor, C. M., and D. H. Kedes. 2006. Mass spectrometric analyses of purified rhesus monkey rhadinovirus reveal 33 virion-associated proteins. J Virol 80:1574-1583.
76. Orzechowska, B. U., M. F. Powers, J. Sprague, H. Li, B. Yen, R. P. Searles, M. K. Axthelm, and S. W. Wong. 2008. Rhesus macaque rhadinovirus-associated non-Hodgkin lymphoma: animal model for KSHV-associated malignancies. Blood 112:4227-4234.
77. Parsons, C. H., L. A. Adang, J. Overdevest, C. M. O'Connor, J. R. Taylor, Jr., D. Camerini, and D. H. Kedes. 2006. KSHV targets multiple leukocyte lineages during long-term productive infection in NOD/SCID mice. The Journal of clinical investigation 116:1963-1973.
78. Patel, D., T. Opriessnig, D. A. Stein, P. G. Halbur, X. J. Meng, P. L. Iversen, and Y. J. Zhang. 2008. Peptide-conjugated morpholino oligomers inhibit porcine reproductive and respiratory syndrome virus replication. Antiviral research 77:95-107.
79. Perkins, N. D. 2007. Integrating cell-signalling pathways with NF-kappaB and IKK function. Nature reviews. Molecular cell biology 8:49-62.
80. Print, C. G., K. L. Loveland, L. Gibson, T. Meehan, A. Stylianou, N. Wreford, D. de Kretser, D. Metcalf, F. Kontgen, J. M. Adams, and S. Cory. 1998. Apoptosis

regulator bcl-w is essential for spermatogenesis but appears otherwise redundant. Proceedings of the National Academy of Sciences of the United States of America 95:12424-12431.

81. Pyo, J. O., M. H. Jang, Y. K. Kwon, H. J. Lee, J. I. Jun, H. N. Woo, D. H. Cho, B. Choi, H. Lee, J. H. Kim, N. Mizushima, Y. Oshumi, and Y. K. Jung. 2005. Essential roles of Atg5 and FADD in autophagic cell death: dissection of autophagic cell death into vacuole formation and cell death. The Journal of biological chemistry 280:20722-20729.
82. Qin, H., S. M. Srinivasula, G. Wu, T. Fernandes-Alnemri, E. S. Alnemri, and Y. Shi. 1999. Structural basis of procaspase-9 recruitment by the apoptotic protease-activating factor 1. Nature 399:549-557.
83. Rajawat, Y., Z. Hilioti, and I. Bossis. 2011. Retinoic Acid Induces Autophagosome Maturation Through Redistribution of the Cation-Independent Mannose-6-Phosphate Receptor. Antioxidants & redox signaling.
84. Rappoport, J. Z. 2008. Focusing on clathrin-mediated endocytosis. The Biochemical journal 412:415-423.
85. Ravikumar, B., Z. Berger, C. Vacher, C. J. O'Kane, and D. C. Rubinsztein. 2006. Rapamycin pre-treatment protects against apoptosis. Human molecular genetics 15:1209-1216.
86. Renne, R., D. Dittmer, D. Kedes, K. Schmidt, R. C. Desrosiers, P. A. Luciw, and D. Ganem. 2004. Experimental transmission of Kaposi's sarcoma-associated herpesvirus (KSHV/HHV-8) to SIV-positive and SIV-negative rhesus macaques. Journal of medical primatology 33:1-9.
87. Renne, R., W. Zhong, B. Herndier, M. McGrath, N. Abbey, D. Kedes, and D. Ganem. 1996. Lytic growth of Kaposi's sarcoma-associated herpesvirus (human herpesvirus 8) in culture. Nature medicine 2:342-346.
88. Sadagopan, S., N. Sharma-Walia, M. V. Veettil, H. Raghu, R. Sivakumar, V. Bottero, and B. Chandran. 2007. Kaposi's sarcoma-associated herpesvirus induces sustained NF-kappaB activation during de novo infection of primary human dermal microvascular endothelial cells that is essential for viral gene expression. J Virol 81:3949-3968.
89. Savill, J., and V. Fadok. 2000. Corpse clearance defines the meaning of cell death. Nature 407:784-788.
90. Schultz, E. R., G. W. Rankin, Jr., M. P. Blanc, B. W. Raden, C. C. Tsai, and T. M. Rose. 2000. Characterization of two divergent lineages of macaque rhadinoviruses related to Kaposi's sarcoma-associated herpesvirus. Journal of virology 74:4919-4928.
91. Searles, R. P., E. P. Bergquam, M. K. Axthelm, and S. W. Wong. 1999. Sequence and genomic analysis of a Rhesus macaque rhadinovirus with similarity to Kaposi's sarcoma-associated herpesvirus/human herpesvirus 8. Journal of virology 73:3040-3053.
92. Shibata, M., T. Lu, T. Furuya, A. Degterev, N. Mizushima, T. Yoshimori, M. MacDonald, B. Yankner, and J. Yuan. 2006. Regulation of intracellular accumulation of mutant Huntingtin by Beclin 1. The Journal of biological chemistry 281:14474-14485.

93. Shukla, D., M. C. Dal Canto, C. L. Rowe, and P. G. Spear. 2000. Striking similarity of murine nectin-1alpha to human nectin-1alpha (HveC) in sequence and activity as a glycoprotein D receptor for alphaherpesvirus entry. Journal of virology 74:11773-11781.
94. Shukla, D., and P. G. Spear. 2001. Herpesviruses and heparan sulfate: an intimate relationship in aid of viral entry. The Journal of clinical investigation 108:503-510.
95. Sieczkarski, S. B., and G. R. Whittaker. 2002. Dissecting virus entry via endocytosis. The Journal of general virology 83:1535-1545.
96. Spear, P. G., R. J. Eisenberg, and G. H. Cohen. 2000. Three classes of cell surface receptors for alphaherpesvirus entry. Virology 275:1-8.
97. Spear, P. G., and R. Longnecker. 2003. Herpesvirus entry: an update. Journal of virology 77:10179-10185.
98. Strasser, A. 2005. The role of BH3-only proteins in the immune system. Nature reviews. Immunology 5:189-200.
99. Sun, Q., H. Matta, and P. M. Chaudhary. 2003. The human herpes virus 8-encoded viral FLICE inhibitory protein protects against growth factor withdrawal-induced apoptosis via NF-kappa B activation. Blood 101:1956-1961.
100. Sun, Q., S. Zachariah, and P. M. Chaudhary. 2003. The human herpes virus 8-encoded viral FLICE-inhibitory protein induces cellular transformation via NF-kappaB activation. J Biol Chem 278:52437-52445.
101. Thome, M., P. Schneider, K. Hofmann, H. Fickenscher, E. Meinl, F. Neipel, C. Mattmann, K. Burns, J. L. Bodmer, M. Schroter, C. Scaffidi, P. H. Krammer, M. E. Peter, and J. Tschopp. 1997. Viral FLICE-inhibitory proteins (FLIPs) prevent apoptosis induced by death receptors. Nature 386:517-521.
102. Thorburn, J., F. Moore, A. Rao, W. W. Barclay, L. R. Thomas, K. W. Grant, S. D. Cramer, and A. Thorburn. 2005. Selective inactivation of a Fas-associated death domain protein (FADD)-dependent apoptosis and autophagy pathway in immortal epithelial cells. Molecular biology of the cell 16:1189-1199.
103. Thurau, M., G. Marquardt, N. Gonin-Laurent, K. Weinlander, E. Naschberger, R. Jochmann, K. R. Alkharsah, T. F. Schulz, M. Thome, F. Neipel, and M. Sturzl. 2009. Viral inhibitor of apoptosis vFLIP/K13 protects endothelial cells against superoxide-induced cell death. Journal of virology 83:598-611.
104. Tsujimoto, Y., and S. Shimizu. 2005. Another way to die: autophagic programmed cell death. Cell death and differentiation 12 Suppl 2:1528-1534.
105. Vaux, D. L., S. Cory, and J. M. Adams. 1988. Bcl-2 gene promotes haemopoietic cell survival and cooperates with c-myc to immortalize pre-B cells. Nature 335:440-442.
106. Vousden, K. 1993. Interactions of human papillomavirus transforming proteins with the products of tumor suppressor genes. The FASEB journal : official publication of the Federation of American Societies for Experimental Biology 7:872-879.
107. Warden, C., Q. Tang, and H. Zhu. 2011. Herpesvirus BACs: past, present, and future. Journal of biomedicine & biotechnology 2011:124595.
108. Wei, M. C., W. X. Zong, E. H. Cheng, T. Lindsten, V. Panoutsakopoulou, A. J. Ross, K. A. Roth, G. R. MacGregor, C. B. Thompson, and S. J. Korsmeyer. 2001.

Proapoptotic BAX and BAK: a requisite gateway to mitochondrial dysfunction and death. Science 292:727-730.
109. Wen, H. J., Z. Yang, Y. Zhou, and C. Wood. 2010. Enhancement of autophagy during lytic replication by the Kaposi's sarcoma-associated herpesvirus replication and transcription activator. J Virol 84:7448-7458.
110. Westmoreland, S. V., and K. G. Mansfield. 2008. Comparative pathobiology of Kaposi sarcoma-associated herpesvirus and related primate rhadinoviruses. Comp Med 58:31-42.
111. White, E. 2008. Autophagic cell death unraveled: Pharmacological inhibition of apoptosis and autophagy enables necrosis. Autophagy 4:399-401.
112. Wong, S. W., E. P. Bergquam, R. M. Swanson, F. W. Lee, S. M. Shiigi, N. A. Avery, J. W. Fanton, and M. K. Axthelm. 1999. Induction of B cell hyperplasia in simian immunodeficiency virus-infected rhesus macaques with the simian homologue of Kaposi's sarcoma-associated herpesvirus. J Exp Med 190:827-840.
113. Wu, Y. T., H. L. Tan, Q. Huang, Y. S. Kim, N. Pan, W. Y. Ong, Z. G. Liu, C. N. Ong, and H. M. Shen. 2008. Autophagy plays a protective role during zVAD-induced necrotic cell death. Autophagy 4:457-466.
114. Young, L. S., and A. B. Rickinson. 2004. Epstein-Barr virus: 40 years on. Nature reviews. Cancer 4:757-768.
115. Yu, L., A. Alva, H. Su, P. Dutt, E. Freundt, S. Welsh, E. H. Baehrecke, and M. J. Lenardo. 2004. Regulation of an ATG7-beclin 1 program of autophagic cell death by caspase-8. Science 304:1500-1502.
116. Yuan, J., S. Shaham, S. Ledoux, H. M. Ellis, and H. R. Horvitz. 1993. The C. elegans cell death gene ced-3 encodes a protein similar to mammalian interleukin-1 beta-converting enzyme. Cell 75:641-652.
117. Zhang, W., F. Zhou, W. Greene, and S. J. Gao. 2010. Rhesus rhadinovirus infection of rhesus fibroblasts occurs through clathrin-mediated endocytosis. Journal of virology 84:11709-11717.